

Quantifying the impact of a periodic presence of antimicrobial on resistance evolution in a homogeneous microbial population of fixed size

Loïc Marrec¹, Anne-Florence Bitbol^{1*}

¹ Sorbonne Université, CNRS, Laboratoire Jean Perrin (UMR 8237), F-75005 Paris, France

* anne-florence.bitbol@sorbonne-universite.fr

Abstract

The evolution of antimicrobial resistance generally occurs in an environment where antimicrobial concentration is variable, which has dramatic consequences on the microorganisms' fitness landscape, and thus on the evolution of resistance.

We investigate the effect of these time-varying patterns of selection within a stochastic model. We consider a homogeneous microbial population of fixed size subjected to periodic alternations of phases of absence and presence of an antimicrobial that stops growth. Combining analytical approaches and stochastic simulations, we quantify how the time necessary for fit resistant bacteria to take over the microbial population depends on the alternation period. We demonstrate that fast alternations strongly accelerate the evolution of resistance, reaching a plateau for sufficiently small periods. Furthermore, this acceleration is stronger in larger populations. For asymmetric alternations, featuring a different duration of the phases with and without antimicrobial, we shed light on the existence of a minimum for the time taken by the population to fully evolve resistance. The corresponding dramatic acceleration of the evolution of antimicrobial resistance likely occurs in realistic situations, and may have an important impact both in clinical and experimental situations.

Introduction

The discovery of antibiotics and antivirals has constituted one of the greatest medical advances of the twentieth century, allowing many major infectious diseases to be treated. However, with the increasing use of antimicrobials, pathogenic microorganisms tend to become resistant to these drugs. Antimicrobial resistance has become a major and urgent problem of public health worldwide [1, 2].

Mutations that confer antimicrobial resistance are often associated with a fitness cost, i.e. a slower reproduction [3–5]. Indeed, the acquisition of resistance generally involves either a modification of the molecular target of the antimicrobial, which often alters its biological function, or the production of specific proteins, which entails a metabolic cost [4]. However, resistant microorganisms frequently acquire subsequent mutations that compensate for the initial cost of resistance. These microorganisms are called “resistant-compensated” [6–9]. The acquisition of resistance is therefore often irreversible, even if the antimicrobial is removed from the environment [4, 6].

In the absence of antimicrobial, the adaptive landscape of the microorganism, which represents its fitness (i.e. its reproduction rate) as a function of its genotype, involves a valley, since the first resistance mutation decreases fitness, while compensatory mutations increase it. However, this fitness valley, which exists in the absence of antimicrobial, disappears above a certain concentration of antimicrobial, as the growth of the antimicrobial-sensitive microorganism is impaired. Thus, the adaptive landscape of the microorganism depends drastically on whether the antimicrobial is present or absent. Taking into account this type of interaction between genotype and environment constitutes a fundamental problem, even though most experiments have traditionally focused on comparing different mutants in a unique environment [10]. In particular, recent theoretical analyses show that variable adaptive landscapes can have a dramatic evolutionary impact [11–15].

How do the timescales of evolution and variation in the adaptive landscape compare and interact? What is the impact of the time variability of the adaptive landscape on the evolution of antimicrobial resistance? In order to answer these questions, we construct a minimal model retaining the fundamental aspects of antimicrobial resistance evolution. Focusing on the case of a homogeneous microbial population of fixed size, we perform a complete stochastic study of *de novo* resistance acquisition in the presence of periodic alternations of phases of absence and presence of an antimicrobial that stops growth. These alternations can represent, for example, a treatment where the concentration within the patient falls under the Minimum Inhibitory Concentration (MIC) between drug intakes [16]. Combining analytical and numerical approaches, we show that these alternations substantially accelerate the evolution of resistance with respect to the cases of continuous absence or continuous presence of antimicrobial, especially for larger populations. We fully quantify this effect and shed light on the different regimes at play. For asymmetric alternations, featuring a different duration of the phases with and without antimicrobial, we demonstrate the existence of a minimum for the time taken by the population to fully evolve resistance, occurring when both phases have durations of the same order. This realistic situation dramatically accelerates the evolution of resistance. Finally, we discuss the implications of our findings, in particular regarding antimicrobial dosage.

Model

The action of an antimicrobial drug can be quantified by its MIC, the minimum concentration that stops the growth of a microbial population [4]. We focus on biostatic antimicrobials, which stop microbial growth (vs. biocidal antimicrobials, which kill microorganisms). We model the action of the antimicrobial in a binary way: below the MIC (“absence of antimicrobial”), growth is not affected, while above it (“presence of antimicrobial”), sensitive microorganisms cannot grow at all. The usual steepness of pharmacodynamic curves around the MIC [16] justifies our simple binary approximation, and we also present an analysis of the robustness of this hypothesis (Supplementary Material, Section 6). Within this binary approximation, there are two adaptive landscapes. Assuming that the drug fully stops the growth of sensitive microorganisms, but does not affect that of resistant ones, and considering compensatory mutations that fully restore fitness, these two adaptive landscapes can be described by a single parameter δ , representing the fitness cost of resistance (Fig. 1A). We focus on asexual microorganisms, and fitness simply denotes the division rate of these organisms. The fitness of sensitive microorganisms in the absence of antimicrobials is taken as reference. In this framework, we investigate the impact of a periodic presence of antimicrobial, assuming that the process starts without antimicrobial (Fig. 1B-C).

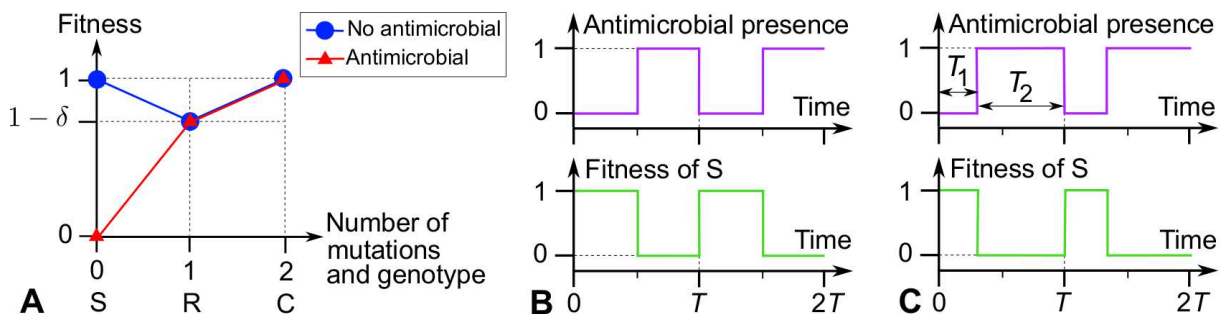


Figure 1: **Model.** (A) Adaptive landscapes in the presence and in the absence of antimicrobial. Genotypes are indicated by the number of mutations from the sensitive microorganism, and by initials: S: sensitive; R: resistant; C: resistant-compensated.

(B) and (C) Periodic presence of antimicrobial, and impact on the fitness of S (sensitive) microorganisms: (B) Symmetric alternations; (C) Asymmetric alternations.

We denote by μ_1 and μ_2 the mutation rates (or mutation probabilities upon each division)

for the mutation from S to R and for the one from R to C, respectively. In several actual situations, the effective mutation rate towards compensation tends to be higher than the one towards the return to sensitivity, since multiple mutations can compensate for the initial cost of resistance [7, 8, 17]. Therefore, we do not take into account back-mutations. Still because of the abundance of possible compensatory mutations, generally $\mu_1 \ll \mu_2$ [7, 18]. We present general analytical results as a function of μ_1 and μ_2 , and analyze in more detail the limit $\mu_1 \ll \mu_2$, especially in simulations. All notations introduced are summed up in Table S1.

We focus on a homogeneous microbial population of fixed size N , which can thus be described in the framework of the Moran process [19, 20], where fitnesses are relative (see Supplementary Material, Section 2 and Fig. S1). Assuming a constant size simplifies the analytical treatment and is appropriate for instance to describe turbidostat experiments, where the dilution rate is adjusted so that turbidity (and hence population size) is constant [21]. If a population only features sensitive individuals (with zero fitness) in the presence of antimicrobial, we consider that no division occurs, and the population remains static. We always express time in number of generations, which corresponds (unless no cell can divide) to the number of Moran steps divided by the population size N .

Throughout, we start from a microbial population where all individuals are S (sensitive), and we focus on the time t_C^f it takes for the C (resistant-compensated) type to fix in the population, i.e. to take over the population. Then, the population has fully evolved resistance *de novo*.

Results

A periodic presence of antimicrobial can drive resistance evolution

In this section, we study how alternations of absence and presence of antimicrobial can drive the *de novo* evolution of resistance. We present analytical predictions for the time needed for the population to evolve resistance, and then we compare them to numerical simulation results.

We first focus on the rare mutation regime $N\mu_1 \ll 1$, where at most one mutant lineage exists in the population at each given time. The frequent mutation regime is briefly discussed, and more detail regarding the appropriate deterministic treatment in this regime is given in Supplementary Material, Section 3. Here, we consider the case of symmetric alternations with period T (Fig. 1B). Asymmetric alternations (Fig. 1C) will be discussed later.

Time needed for resistant microorganisms to start growing

Resistant (R) mutants can only appear during phases without antimicrobial. Indeed, mutations occur upon division, and sensitive (S) bacteria cannot divide in the presence of antimicrobial (Fig. 1). However, R mutants are less fit than S individuals without antimicrobial. Hence, the lineage of an R mutant will very likely disappear, unless it survives until the next addition of antimicrobial. More precisely, without antimicrobial, the fixation probability p_{SR} of a single R mutant with fitness $1 - \delta$, in a population of size N where all other individuals are of type S and have fitness 1, is $\sim 1/N$ if the mutation from S to R is effectively neutral ($N\delta \ll 1$), and $\sim \delta e^{-N\delta}$ if $\delta \ll 1$ and $N\delta \gg 1$ [20]. Let us denote by τ_R^d the average time an R lineage would drift before going extinct without antimicrobial [20] (see Supplementary Material, Section 2). If antimicrobial is added while R mutants exist in the population, i.e. within $\sim \tau_R^d$ after a mutation event, then the R population will grow fast and fix, since S individuals cannot divide with antimicrobial. Hence, each time antimicrobial is added, any R lineage that was destined for extinction without antimicrobial but that survived until the addition of drug is rescued. Through this phenomenon, periodic alternations of absence and presence of antimicrobial can substantially accelerate resistance evolution: we will quantify this effect. Note that here, we disregard the very few R lineages destined for fixation without antimicrobial, because we aim to study the acceleration of resistance evolution due to the alternations. The spontaneous evolution of resistance without antimicrobial is discussed and compared to our alternation-driven process in the Supplementary Material, Section 4.

It is crucial to calculate the average waiting time t_R^a until an R lineage is rescued by the addition of antimicrobial. Indeed, this constitutes the key step of alternation-driven resistance takeover. Three timescales impact t_R^a . The first one is the timescale of the environment, namely the half-period $T/2$. The two other ones are intrinsic timescales of the evolution of the population without antimicrobial: the average time between the appearance of two independent R mutants, $1/(N\mu_1)$, and the average lifetime τ_R^d of the lineage of an R mutant destined for extinction without antimicrobial. Note that τ_R^d is generally quite short. Indeed, $\tau_R^d \approx \log N$ for large N if $\delta = 0$, and τ_R^d decreases as δ increases, as deleterious R mutants are out-competed by S microorganisms; for instance, $\tau_R^d \approx 2.6$ generations if $\delta = 0.1$ in the limit where $N \gg 1$ and $N\delta \gg 1$ [20] (see Supplementary Information, Section 2). Hence, in the rare mutation regime, $\tau_R^d \ll 1/(N\mu_1)$. What matters is how the environment timescale $T/2$ compares to these two evolution timescales (see Fig. 2A-C). Our arguments based on comparing average timescales are approximate, but they yield explicit analytical predictions in each regime where timescales are separated, which we then test through numerical simulations.

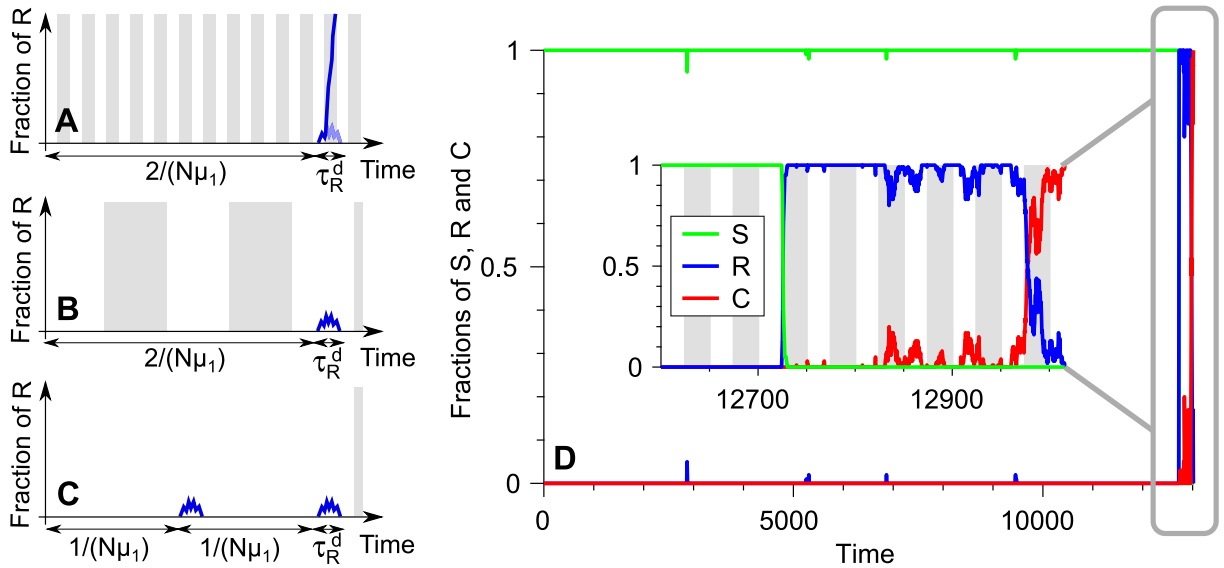


Figure 2: Alternation-driven evolution of antimicrobial resistance. (A-C) Sketches illustrating the three different regimes for the half-period $T/2$ of the alternations of antimicrobial absence (white) and presence (gray). The fraction of resistant (R) microorganisms in the population is plotted versus time (blue curves). R mutants can only appear without antimicrobial. (A) $T/2 \ll \tau_R^d$, where τ_R^d is the average extinction time of the lineage of an R mutant without antimicrobial. The first R lineage that appears is expected to live until the next addition of antimicrobial and is then rescued. (B) $\tau_R^d \ll T/2 \ll 1/(N\mu_1)$, where $1/(N\mu_1)$ is the average time between the appearance of two independent R mutants without antimicrobial. (C) $T/2 \gg 1/(N\mu_1)$. In (B) and (C), not all R lineages live until the next addition of antimicrobial, and in (C) multiple R lineages arise within a half-period. (D) Example of a simulation run. The fractions of S, R and C microorganisms are plotted versus time. Inset: end of the process, with full resistance evolution. As in (A-C), antimicrobial is present during the gray-shaded time intervals (shown only in the inset given their duration). Parameters: $\mu_1 = 10^{-5}$, $\mu_2 = 10^{-3}$, $\delta = 0.1$, $N = 10^2$ and $T = 50$ (belonging to regime B).

(A) If $T/2 \ll \tau_R^d$ (Fig. 2A): The lineage of the first R mutant that appears is likely to still exist upon the next addition of antimicrobial, and to be rescued, which yields $t_R^a = 2/(N\mu_1)$. Indeed, mutations from S to R can only occur without antimicrobial, i.e. half of the time.

(B) If $\tau_R^d \ll T/2 \ll 1/(N\mu_1)$ (Fig. 2B): At most one mutation yielding an R individual is expected within each half-period. The lineage of this mutant is likely to survive until the next addition of antimicrobial only if the mutant appeared within the last $\sim \tau_R^d$ preceding it, which has a probability $p = 2\tau_R^d/T$. Hence, $t_R^a = 2/(N\mu_1 p) = T/(N\mu_1 \tau_R^d)$.

(C) If $T/2 \gg 1/(N\mu_1)$ (Fig. 2C): Since the half-period is much larger than the time $1/(N\mu_1)$ between the appearance of two independent mutants without antimicrobial, several appearances and extinctions of R lineages are expected within one half-period. Hence, the probability that a lineage of R exists upon a given addition of antimicrobial is $q = N\mu_1\tau_R^d$, which corresponds to the fraction of time during which R mutants are present in the phases without antimicrobial. Specifically, q is the ratio of the average lifetime of the lineage of an R mutant destined for extinction without antimicrobial to the average time between the appearance of two independent R mutants without antimicrobial. Since additions of antimicrobial occur every T , we have $t_R^a = T/q = T/(N\mu_1\tau_R^d)$, which is the same as in case (B). In fact, the demonstration presented for case (C) also holds for case (B).

In conclusion, we obtain

$$t_R^a = \frac{T}{N\mu_1 \min(\tau_R^d, T/2)}. \quad (1)$$

Hence, if $T/2 \ll \tau_R^d$, t_R^a is independent from the period T of alternations, while if $T/2 \gg \tau_R^d$, t_R^a is proportional to T .

Time needed for the population to fully evolve resistance

We are interested in the average time t_C^f it takes for the population to fully evolve resistance, i.e. for the C (resistant-compensated) type to fix. An example of the process is shown in Fig. 2D. It takes on average t_R^a for R mutants to be rescued by the addition of antimicrobial. Then they rapidly grow, since S individuals cannot divide. If the phase with antimicrobial is long enough, R mutants take over during this phase, with a probability 1 and an average fixation timescale $\tau_R^f \approx \log N$ for $N \gg 1$ [20] (see Supplementary Material, Section 2). If $T/2 \ll \tau_R^f$, fixation cannot occur within a single half-period, and the R lineage will drift longer, but its extinction remains very unlikely. Indeed, while R individuals are the only ones that can divide with antimicrobial, we assume that they experience only a minor disadvantage without antimicrobial ($1 - \delta$ vs. 1, generally with $\delta \ll 1$ [4], see Fig. 1A). Hence, if $T/2 \ll \tau_R^f$, and neglecting changes in frequencies in the absence of antimicrobial, R mutants will take $\sim 2\tau_R^f$ to fix.

Once the R type has fixed in the population, the appearance and eventual fixation of C mutants are independent from the presence of antimicrobial, since only S microorganisms are affected by it (see Fig. 1A). The first C mutant whose lineage will fix takes an average time $t_C^a = 1/(N\mu_2 p_{RC})$ to appear once R has fixed, where p_{RC} is the fixation probability of a single C mutant in a population of size N where all other individuals are of type R. In particular, if $N\delta \ll 1$ then $p_{RC} = 1/N$, and if $\delta \ll 1$ and $N\delta \gg 1$ then $p_{RC} \approx \delta$ [20] (see Supplementary Material, Section 2). The final step is the fixation of this successful C mutant, which will take an average time τ_C^f , of order N in the effectively neutral regime $N\delta \ll 1$, and shorter for larger δ given the selective advantage of C over R [20] (see Supplementary Material, Section 2). Note that we have assumed for simplicity that the fixation of R occurs before the appearance of the first successful C mutant, which is true if $t_C^a \gg \tau_R^f$, i.e. $1/(N\mu_2 p_{RC}) \gg \log N$. This condition is satisfied if the second mutation is sufficiently rare. Otherwise, our calculation will slightly overestimate the actual result.

Combining the previous results yields

$$t_C^f \approx t_R^a + \tau_R^f + t_C^a + \tau_C^f, \quad (2)$$

where t_R^a is given by Eq. 1, while $t_C^a = 1/(N\mu_2 p_{RC})$, and $\tau_R^f \approx \log N$ and $\tau_C^f \lesssim N$. In the rare mutation regime, the contribution of the two fixation times τ_R^f and τ_C^f will be negligible. If in addition $\mu_1 \ll \mu_2$, which is realistic (cf. Methods), then t_C^f will be dominated by t_R^a . If $\mu_1 \approx \mu_2$, t_C^f will be dominated by t_R^a if $T > \max(2\tau_R^d, \tau_R^d/p_{RC})$. Indeed, if $T < 2\tau_R^d$, using Eq. 1 shows that the condition $t_R^a > t_C^a$ is then equivalent to $p_{RC} > 1/2$, which cannot be satisfied for $\delta \ll 1$. Hence, $T > 2\tau_R^d$ is necessary to have $t_R^a > t_C^a$. But if $T > 2\tau_R^d$ and $\mu_1 \approx \mu_2$, the condition $t_R^a > t_C^a$ is equivalent to $T > \tau_R^d/p_{RC}$. Beyond the regime $T > \max(2\tau_R^d, \tau_R^d/p_{RC})$, the contribution of t_C^a to t_C^f will be important.

Comparison of analytical predictions and simulation results

Fig. 3A shows simulation results for the average total fixation time t_C^f of C individuals in the population. This time is plotted as a function of the period T of alternations for different population sizes N . As predicted above (see Eq. 1), we observe two regimes delimited by $T = 2\tau_R^d$. If $T \ll 2\tau_R^d$, t_C^f does not depend on T , while if $T \gg 2\tau_R^d$, it depends linearly on T . In Fig. 3A, we also plot our analytical prediction from Eqs. 1 and 2 in these two regimes (solid lines). The agreement with our simulated data is excellent for small and intermediate values of T , without any adjustable parameter. Interestingly, the transition between these two regimes occurs for periods of about 5 generations, which would correspond to a few hours for typical bacteria, thus highlighting the practical importance of these two regimes. In Fig. 3A, the smallest values reported for t_C^f are of order 100 generations, corresponding to a few days, and are thus relevant to an actual treatment, while some other values are larger than the timescales involved in a treatment. Here, we quantitatively analyze the phenomena for a wide range of parameters. A more detailed comparison to actual situations, employing realistic values of population sizes and mutation rates, is presented in the Discussion.

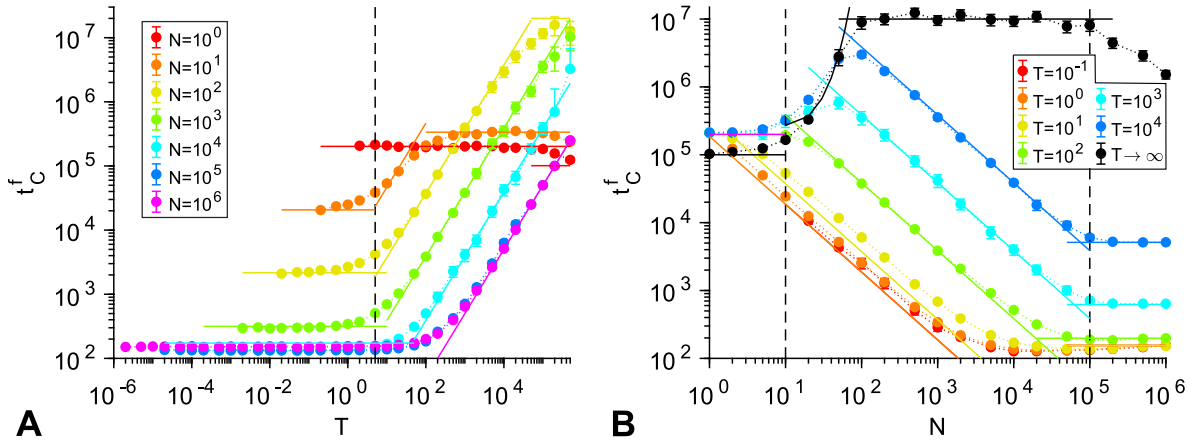


Figure 3: **Impact of symmetric alternations.** Fixation time t_C^f of C (resistant-compensated) individuals in a population of N individuals subjected to symmetric alternations of absence and presence of antimicrobial with period T . Data points correspond to the average of simulation results, and error bars (often smaller than markers) represent 95% confidence intervals. 2 to 10^4 replicate simulations were performed in each case (the smallest numbers of replicates were used for the largest populations, whose evolution is quasi-deterministic). In both panels, solid lines correspond to our analytical predictions in each regime. Parameter values: $\mu_1 = 10^{-5}$, $\mu_2 = 10^{-3}$, and $\delta = 0.1$. (A) t_C^f as function of T . Vertical dashed line: $T = 2\tau_R^d$. (B) t_C^f as function of N . Left vertical dashed line: limit of the neutral regime, $N = 1/\delta$. Right vertical dashed line: limit of the deterministic regime, $N = 1/\mu_1$. Horizontal purple line: analytical prediction for valley crossing by neutral tunneling in the presence of alternations (see Supplementary Material, Section 4). Black lines: analytical predictions for fitness valley crossing times in the absence of alternations (see Supplementary Material, Section 4).

Importantly, Fig. 3A shows that t_C^f reaches a plateau for small N and large T , which is not predicted by our analysis of the alternation-driven evolution of resistance. This plateau corresponds to the spontaneous fitness valley crossing process [22], through which resistance mutations appear and fix in the absence of drug. Note that such a plateau would also be reached for larger N , but for periods T longer than those considered in Fig. 3A (see Fig. 3B, black lines). What ultimately matters is the shortest process among the alternation-driven one and the spontaneous valley-crossing one. In Fig. 3A, horizontal solid lines at large T represent our analytical predictions for the valley-crossing time (see Supplementary Material, Section 4).

Fig. 3B shows simulation results for t_C^f as function of N for different T . Again, solid lines rep-

resent our analytical predictions from Eqs. 1 and 2, yielding excellent agreement for intermediate values of N , and for small ones at small T . In other regimes, resistance evolution is achieved by spontaneous valley crossing. In the limit $T \rightarrow \infty$ of continuous absence of antimicrobial (black data points in Fig. 3B), only valley crossing can occur, and the black solid lines correspond to our analytical predictions for this process (see Supplementary Material, Section 4).

Until now, we focused on the rare mutation regime. In the large-population, frequent-mutation regime $N \gg 1/\mu_1 \gg 1$, the dynamics of the population can be well-approximated by a deterministic model with replicator-mutator differential equations [23, 24] (see Supplementary Material, Section 3). Then, several lineages of mutants can coexist. If $T/2 \gg 1/(N\mu_1)$, it is almost certain that some R mutants exist in the population upon the first addition of antimicrobial, which entails $t_R^a = T/2$. The horizontal purple solid line plotted at large T in Fig. 3A, and the horizontal solid lines at large N in Fig. 3B, both correspond to this deterministic prediction. In the Supplementary Material, Section 3, we study the deterministic limit of our stochastic model, and demonstrate that it matches the results obtained in Fig. 3A for $N = 10^5$ and $N = 10^6$ over the whole range of T (see Fig. S2).

The comparison to the spontaneous fitness valley crossing process (Fig. 3B, black curve and Supplementary Material, Section 4) demonstrates that periodic alternations of absence and presence of antimicrobial can dramatically accelerate resistance evolution compared to continuous absence of antimicrobial. Recall that within our model, sensitive microorganisms cannot divide with antimicrobial, so resistance cannot evolve at all in continuous presence of antimicrobial. Another possible comparison would be to a continuous presence of a low dose of antimicrobial (below the MIC), but this goes beyond our binary model of antimicrobial action (see Supplementary Information, Section 6 for a discussion of the domain of validity of this model). Alternations are really essential: R mutants appear without antimicrobial, and each addition of antimicrobial rescues the existing R lineages that would be destined to extinction without antimicrobial.

Asymmetric alternations

We now turn to the more general case of asymmetric alternations of phases of absence and presence of antimicrobial, with respective durations T_1 and T_2 , and $T = T_1 + T_2$ (see Fig. 1C).

The average time t_R^a when R mutants first exist in the presence of antimicrobial, and start growing, can be obtained by a straightforward generalization of the symmetric alternation case Eq. 1. What matters is how the duration T_1 of the phase without antimicrobial, where S individuals can divide and mutate, compares to the average time τ_R^d an R lineage would drift before extinction without antimicrobial. If $T_1 \ll \tau_R^d$, the first R mutant takes an average time $T/(N\mu_1 T_1)$ to appear, and is likely to be rescued by the next addition of antimicrobial. If $T_1 \gg \tau_R^d$, the fraction of time during which R mutants are present in the phases without antimicrobial is $N\mu_1 \tau_R^d$, and antimicrobial is added every T , so $t_R^a = T/(N\mu_1 \tau_R^d)$. Hence, we obtain

$$t_R^a = \frac{T}{N\mu_1 \min(\tau_R^d, T_1)}. \quad (3)$$

Once the R mutants have taken over the population, the appearance and fixation of C mutants is not affected by the alternations. Hence, Eq. 2 holds for asymmetric alternations, with t_R^a given by Eq. 3. In the rare mutation regime, if $\mu_1 \ll \mu_2$, then t_C^f will be dominated by t_R^a , and if $\mu_1 \approx \mu_2$, then t_C^f will be dominated by t_R^a if $T > \min(\tau_R^d, T_1)/p_{RC}$, where p_{RC} is the fixation probability of a single C mutant in a population of R individuals.

Fig. 4A shows simulation results for t_C^f as a function of the duration T_1 of the phases without antimicrobial, for different values of the duration T_2 of the phases with antimicrobial. As predicted above, we observe a transition at $T_1 = \tau_R^d$, and different behaviors depending whether $T_2 \ll \tau_R^d$ or $T_2 \gg \tau_R^d$. Our analytical predictions from Eqs. 2 and 3 are plotted in Fig. 4A in the various regimes (solid lines), and are in excellent agreement with the simulation data. The plateau of t_C^f at large T_1 corresponds to spontaneous valley crossing, and the analytical prediction (see Supplementary Material, Section 4) is plotted in black in Fig. 4A.

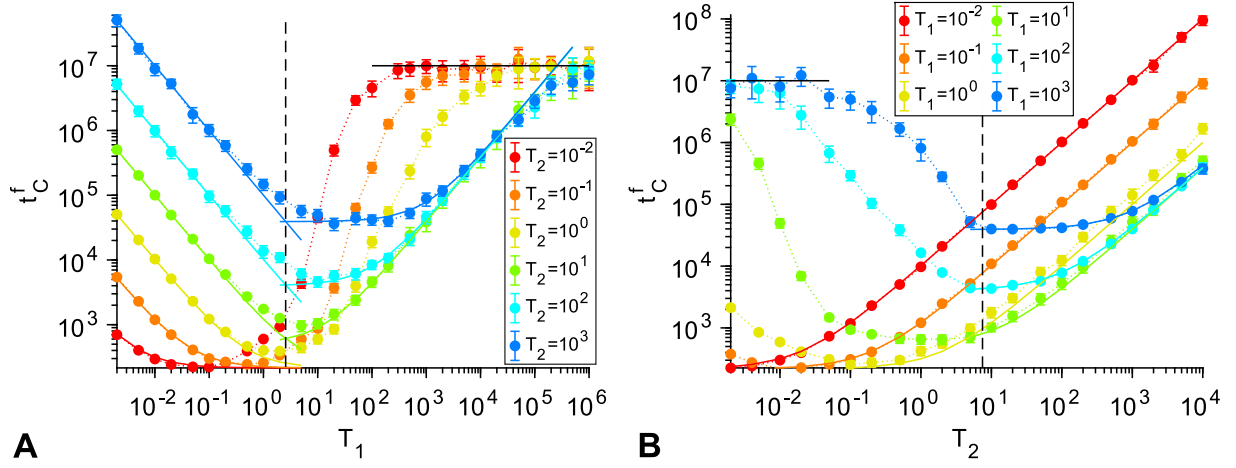


Figure 4: **Asymmetric alternations.** Fixation time t_C^f of C individuals in a population subjected to asymmetric alternations of absence and presence of antimicrobial (respective durations: T_1 and T_2). Data points correspond to the average of simulation results (over 10 to 10^3 replicates), and error bars (sometimes smaller than markers) represent 95% confidence intervals. In both panels, solid lines correspond to our analytical predictions in each regime. In particular, black lines are analytical predictions for fitness valley crossing times in the absence of alternations (see Supplementary Material, Section 4). Parameter values: $\mu_1 = 10^{-5}$, $\mu_2 = 10^{-3}$, $\delta = 0.1$ and $N = 10^3$. (A) t_C^f as function of T_1 for different T_2 . Dashed line: $T_1 = \tau_R^d$. (B) t_C^f as function of T_2 for different T_1 . Dashed line: $T_2 = \tau_R^f$.

For $T_2 \gg \tau_R^f$, Fig. 4A shows that t_C^f features a striking minimum, which gets higher but wider for longer T_2 . This can be fully understood from our analytical predictions. Indeed, when T_1 is varied starting from small values at fixed $T_2 \gg \tau_R^f$, different regimes can be distinguished:

- When $T_1 \ll \tau_R^d$ ($\lesssim \tau_R^f \ll T_2$), Eq. 3 yields $t_R^a = T/(N\mu_1 T_1) \approx T_2/(N\mu_1 T_1) \propto 1/T_1$.
- When $\tau_R^d \ll T_1 \ll T_2$, Eq. 3 gives $t_R^a = T/(N\mu_1 \tau_R^d) \approx T_2/(N\mu_1 \tau_R^d)$, which is independent from T_1 .
- As T_1 reaches and exceeds T_2 , the law $t_R^a = T/(N\mu_1 \tau_R^d)$ still holds. It yields $t_R^a \approx T_1/(N\mu_1 \tau_R^d) \propto T_1$ when $\tau_R^d \ll T_2 \ll T_1$.

Hence, the minimum of t_R^a is $T_2/(N\mu_1 \tau_R^d) \propto T_2$ and is attained for $\tau_R^d \ll T_1 \ll T_2$: it gets higher but wider for larger T_2 .

In the opposite regime where $T_2 \ll \tau_R^d \lesssim \tau_R^f$, Fig. 4A shows that t_C^f also features a minimum as a function of T_1 :

- When $T_1 \ll T_2 \ll \tau_R^d$, Eq. 3 yields $t_R^a = T/(N\mu_1 T_1) \approx T_2/(N\mu_1 T_1) \propto 1/T_1$.
- When $T_2 \ll T_1 \ll \tau_R^d$, the same law gives $t_R^a = T/(N\mu_1 T_1) \approx 1/(N\mu_1)$, which is independent from T_1 .
- When $T_2 \ll \tau_R^d \ll T_1$, R lineages eventually tend to go extinct, even once they have started growing thanks to an addition of antimicrobial (see Supplementary Material, Section 5 and Fig. S3B). Then, alternations do not accelerate resistance evolution, and spontaneous valley crossing dominates (black horizontal line in Fig 4A).

Hence, the minimum of t_R^a is $1/(N\mu_1)$ and is attained for $T_2 \ll T_1 \ll \tau_R^d$: then, the first R mutant that appears is likely to be rescued by the next addition of antimicrobial, thus driving the complete evolution of resistance in the population. For $T_2 \leq T_1 \ll \tau_R^d$, t_R^a is between once and twice this minimum value.

A similar analysis can be conducted if T_2 is varied at fixed T_1 (Fig. 4B); it is presented in the Supplementary Material, Section 5. In a nutshell, for asymmetric alternations, a striking minimum for the time of full evolution of resistance by a population occurs when both phases have durations of the same order. Interestingly, the minimum generally occurs when the phases of antimicrobial presence are shorter than those of absence, i.e. $T_2 \leq T_1$ (except if $T_2 \gg \tau_R^d$).

In addition to this minimum, Fig. 4 also shows a regime of parameters, when $T_1 \ll T_2$ and $T_1 \ll \tau_R^d$, where the evolution of resistance actually takes longer than fitness valley crossing in the absence of antimicrobial (black lines in Fig. 4). Comparing the timescales involved (see Supplementary Material, Section 4) shows that in this regime, if $T_2 \gg T_1 \delta / \mu_2$, the alternation-driven process is faster than the valley-crossing process in the presence of alternations, and thus dominates, but it is slower than the valley-crossing process in the absence of antimicrobial. Hence, in this case, the drug actually slows down the evolution of resistance. Qualitatively, this is because the antimicrobial prevents mutants from arising when it is present.

Discussion

Main conclusions

Because of the generic initial fitness cost of resistance mutations, alternations of phases of absence and presence of antimicrobial induce a dramatic time variability of the adaptive landscape associated to resistance evolution, which alternates back and forth from a fitness valley to an ascending landscape. Using a general and minimal theoretical model which retains the key biological ingredients, we have shed light on the quantitative implications of these time-varying patterns of selection on the time it takes for resistance to fully evolve *de novo* in a homogeneous microbial population of fixed size. Combining analytical approaches and simulations, we showed that resistance evolution can be driven by periodic alternations of phases of absence and presence of an antimicrobial that stops growth. Indeed, the addition of antimicrobial is able to rescue resistant lineages that were destined to go extinct without antimicrobial.

We found that fast alternations strongly accelerate the evolution of resistance. In the limit of short alternation periods, the very first resistant mutant that appears is likely to ultimately lead to full resistance of the population, as it will generally be rescued by the next addition of antimicrobial before going extinct, which would be its most likely fate without antimicrobial. For larger periods T , the time needed for resistance to evolve increases linearly with T , until it reaches the spontaneous valley-crossing time with alternations, which constitutes an upper bound. Our complete stochastic model allowed us to investigate the impact of population size N , beyond the limit $N \gg 1/\mu_1$ addressed by deterministic models. We showed that the acceleration of resistance evolution is stronger for larger populations, eventually reaching a plateau in the deterministic limit. Over a large range of intermediate parameters, the time needed for the population to fully evolve resistance scales as T/N . These results are summed up in Fig. 5A.

For asymmetric alternations, featuring different durations T_1 and T_2 of the phases of absence and presence of antimicrobial, we have shed light on the existence of a minimum for the time taken by the population to fully evolve resistance. This striking minimum occurs when both phases have durations of the same order, generally with $T_1 \leq T_2$. Moreover, the minimum value reached for the time of resistance evolution decreases for shorter alternation periods. These results are summed up in Fig. 5B.

Context and perspectives

Our approach is complementary to previous studies providing a detailed modeling of specific treatments [16, 25–30]. Indeed, the majority of them [16, 25–28, 31, 32] neglect stochastic effects, while they can have a crucial evolutionary impact [20, 33]. The deterministic approach is appropriate if the number N of competing microbes satisfies $N\mu_1 \gg 1$, where μ_1 is the mutation rate [33, 34]. Such large sizes can be reached in some established infections [17], but microbial populations go through very small bottleneck sizes (sometimes $N \sim 1-10$ [35]) when an infection

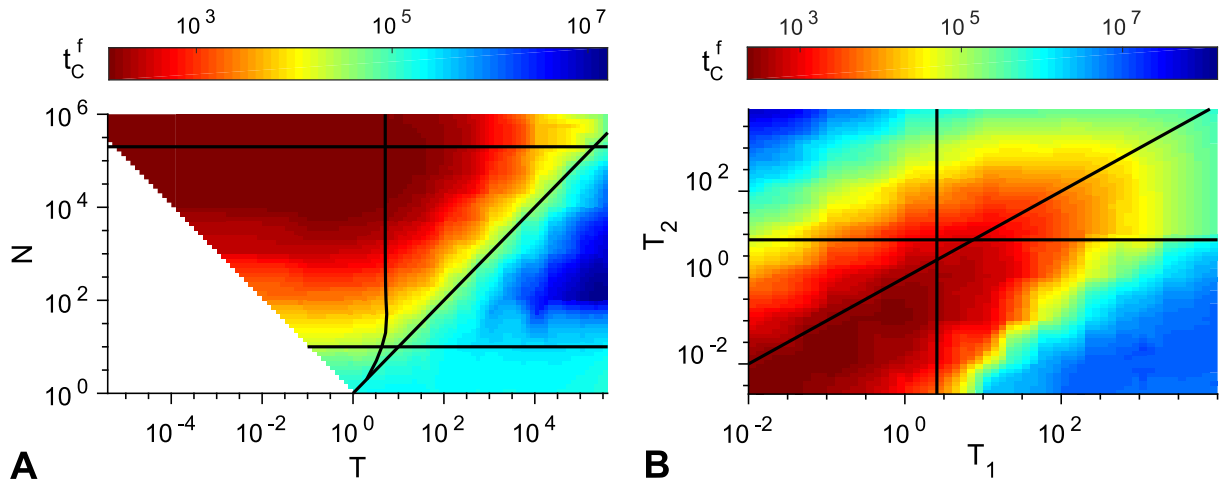


Figure 5: **Heatmaps.** Fixation time t_C^f of C individuals in a population of size N subjected to periodic alternations of absence and presence of antimicrobial. Simulation data plotted in Figs. 3A and 4A are linearly interpolated. Parameter values: $\mu_1 = 10^{-5}$, $\mu_2 = 10^{-3}$, $\delta = 0.1$. (A) Symmetric alternations: t_C^f as function of the period T and the population size N . Top horizontal line: deterministic regime limit $N = 1/\mu_1$. Bottom horizontal line: neutral regime limit $N = 1/\delta$. Quasi-vertical curve: $T = 2\tau_R^d$. Diagonal line: $T = N$. Note that no data is shown for $T/2 < 1/N$ because of the discreteness of our model, which can only deal with timescales larger or equal to the duration of one Moran step, i.e. $1/N$ generation. (B) Asymmetric alternations: t_C^f as function of the durations T_1 and T_2 of the phases of absence and presence of antimicrobial. Vertical line: $T_1 = \tau_R^d$. Horizontal line: $T_2 = \tau_R^f$. Diagonal line: $T_1 = T_2$. Here $N = 10^3$, so the first resistant mutant appears after an average time $T/(N\mu_1 T_1) = 10^2 T/T_1$.

is transmitted. Moreover, established microbial populations are structured, even within a single patient [36], and competition is local, which decreases the effective value of N . Some previous studies did take stochasticity into account, but several did not include compensation of the cost of resistance [37, 38], while others made specific epidemiological assumptions [29].

Given the usual steepness of pharmacodynamic curves [16], we have modeled the action of a biostatic antimicrobial in a binary way, with no growth inhibition under the MIC and full growth inhibition of S microorganisms above it (see Model). An analysis of the robustness of this approximation is presented in the Supplementary Material, Section 6, showing that it is appropriate if the rise time, i.e. the time needed for the fitness of sensitive microorganisms to switch from a low value to a high value and vice-versa when antimicrobial is removed or added, is short enough (see Fig. S4). Qualitatively, if this rise time is shorter than the other environmental and evolutionary timescales at play, then the fitness versus time function is effectively binary.

Our model assumes that the size of the microbial population remains constant. While this is realistic in some controlled experimental setups, e.g. turbidostats [21], microbial populations involved in infections tend to grow, starting from a small transmission bottleneck, and the aim of the antimicrobial treatment is to make them decrease in size and eventually go extinct. In the case of biostatic antimicrobials, which prevent bacteria from growing, populations can go extinct due to spontaneous and immune system-induced death. Our model with constant population size should however be qualitatively relevant at the beginning and middle stages of a treatment (i.e. sufficiently after transmission and before extinction). Constant population sizes facilitate analytical calculations, and allowed us to fully quantify the impact of a periodic presence of antimicrobial on resistance evolution, but it will be very interesting to extend our work to variable population sizes [13, 39, 40]. This would allow us to model biocidal antimicrobials, and to include effects such as antibiotic tolerance, which tend to precede resistance under intermittent antibiotic exposure [41]. Another exciting extension would be to incorporate spatial structure [42–44] and environment heterogeneity, in particular drug concentration gradients. Indeed, static gradients

can strongly accelerate resistance evolution [45–48], and one may ask how this effect combines with the temporal alternation-driven one investigated here. Besides, it would be interesting to compare the impact of periodic alternations to that of random switches of the environment [11–15].

Implications for clinical and experimental situations

The situation where the phases of absence and presence of antimicrobial have similar durations ($T_1 \approx T_2$) yields a dramatic acceleration of resistance evolution, and is unfortunately clinically realistic. Indeed, a goal in treatment design is that the serum concentration of antimicrobial exceeds the MIC for at least 40 to 50% of the time [49], which implies that actual treatments may involve the alternations that most favor resistance evolution according to our results [16, 49]. Besides, bacteria divide on a timescale of about an hour (yielding a τ_R^d of order of a few hours), and antimicrobial is often taken every 8 to 12 hours in treatments by the oral route, so the alternation period does not last for many generations: this is close to our worst-case scenario of short symmetric periods.

In this worst case scenario, full *de novo* resistance evolution can result from the appearance of the very first R mutant, which takes $T/(N\mu_1T_1)$. Indeed, its lineage is likely to be rescued by the next addition of antimicrobial. Under the conservative assumption that only one resistance mutation is accessible, taking $\mu_1 \sim 10^{-10}$, which is the typical mutation probability per nucleotide and per generation in *Escherichia coli* bacteria [50], and taking $\delta \sim 0.1$ [6], we find that this duration is less than a day ($\sim 10 - 20$ generations) for $N \sim 10^9$, and a few days for $N \sim 10^8$, numbers that can be reached in infections [5, 17]. For such large populations, the fixation of the C (compensated) mutant will take more time, but once R is fixed (which takes ~ 1 day after the appearance of the first R mutant), C is very likely to fix even if the treatment is stopped. This is due to the large number of compensatory mutations, which yields a much higher effective mutation rate toward compensation than toward reversion to sensitivity [7, 8, 17]. In addition, many mutations to resistance are often accessible, yielding higher effective μ_1 , e.g. $\mu_1 \sim 10^{-8}$ for rifampicin resistance in some wild isolates of *E. coli* [9], meaning that smaller populations can also quickly become resistant in the presence of alternations. Recall that we are only considering *de novo* resistance evolution, without pre-existent resistant mutants, or other possible sources of resistance, such as horizontal gene transfer, which would further accelerate resistance acquisition.

In summary, an antimicrobial concentration that drops below the MIC between each intake can dramatically favor *de novo* resistance evolution. More specifically, we showed that the worst case occurs when $T_1 \leq T_2$, which would be the case if the antimicrobial concentration drops below the MIC relatively briefly before each new intake. Our results thus emphasize how important it is to control for such apparently innocuous cases, and constitute a striking argument in favor of the development of extended-release antimicrobial formulations [51].

While the parameter range that strongly accelerates resistance evolution should preferably be avoided in clinical situations, it could be tested and harnessed in evolution experiments. Again, these parameters are experimentally accessible. Controlled variations of antimicrobial concentration are already used experimentally, in particular in morbidostat experiments [52], where the population size is kept almost constant, which matches our model. In Ref. [52], a dramatic and reproducible evolution of resistance was observed in ~ 20 days when periodically adjusting the drug concentration to constantly challenge *E. coli* bacteria. Given our results, it would be interesting to test whether resistance evolution could be made even faster by adding drug in a turbidostat with a fixed periodicity satisfying $T_1 \leq T_2 \ll \tau_R^d$.

Acknowledgments

We thank Claude Loverdo, David J. Schwab and Raphaël Voituriez for stimulating discussions. AFB also acknowledges the KITP Program on Evolution of Drug Resistance (KITP, Santa

Barbara, CA, 2014), which was supported in part by the National Science Foundation under Grant NSF PHY 17-48958. LM acknowledges funding by a graduate fellowship from EDPIF.

References

- [1] World Health Organization. Antimicrobial resistance: global report on surveillance; 2014.
- [2] UK Review on Antimicrobial Resistance, chaired by Jim O’Neill, 2016;.
- [3] Borman AM, Paulous S, Clavel F. Resistance of human immunodeficiency virus type 1 to protease inhibitors: selection of resistance mutations in the presence and absence of the drug. *J Gen Virol.* 1996 Mar;77 (Pt 3):419–426.
- [4] Andersson DI, Hughes D. Antibiotic resistance and its cost: is it possible to reverse resistance? *Nat Rev Microbiol.* 2010;8:260–271.
- [5] zur Wiesch PA, Kouyos R, Engelstadter J, Regoes RR, Bonhoeffer S. Population biological principles of drug-resistance evolution in infectious diseases. *Lancet Infect Dis.* 2011 Mar;11(3):236–247.
- [6] Schrag SJ, Perrot V, Levin BR. Adaptation to the fitness cost of antibiotic resistance in *E. coli*. *Proc R Soc Lond B.* 1997;264:1287–1291.
- [7] Levin BR, Perrot V, Walker N. Compensatory mutations, antibiotic resistance and the population genetics of adaptive evolution in bacteria. *Genetics.* 2000 Mar;154(3):985–997.
- [8] Paulander W, Maisnier-Patin S, Andersson DI. Multiple mechanisms to ameliorate the fitness burden of mupirocin resistance in *Salmonella typhimurium*. *Mol Microbiol.* 2007 May;64(4):1038–1048.
- [9] Moura de Sousa J, Sousa A, Bourgard C, Gordo I. Potential for adaptation overrides cost of resistance. *Future Microbiol.* 2015;10(9):1415–1431.
- [10] Taute KM, Gude S, Nghe P, Tans SJ. Evolutionary constraints in variable environments, from proteins to networks. *Trends Genet.* 2014 May;30(5):192–198.
- [11] Mustonen V, Lässig M. Molecular evolution under fitness fluctuations. *Phys Rev Lett.* 2008 Mar;100(10):108101.
- [12] Rivoire O, Leibler S. The Value of Information for Populations in Varying Environments. *J Stat Phys.* 2011;142:1124–1166.
- [13] Melbinger A, Vergassola M. The Impact of Environmental Fluctuations on Evolutionary Fitness Functions. *Sci Rep.* 2015 Oct;5:15211.
- [14] Desponds J, Mora T, Walczak AM. Fluctuating fitness shapes the clone-size distribution of immune repertoires. *Proc Natl Acad Sci USA.* 2016 Jan;113(2):274–279.
- [15] Wienand K, Frey E, Mobilia M. Evolution of a fluctuating population in a randomly switching environment. *Phys Rev Lett.* 2017 Oct;119(15):158301.
- [16] Regoes RR, Wiuff C, Zappala RM, Garner KN, Baquero F, Levin BR. Pharmacodynamic functions: a multiparameter approach to the design of antibiotic treatment regimens. *Antimicrob Agents Chemother.* 2004 Oct;48(10):3670–3676.
- [17] Hughes D, Andersson DI. Evolutionary consequences of drug resistance: shared principles across diverse targets and organisms. *Nat Rev Genet.* 2015 Aug;16(8):459–471.

- [18] Poon A, Davis BH, Chao L. The coupon collector and the suppressor mutation: estimating the number of compensatory mutations by maximum likelihood. *Genetics*. 2005 Jul;170(3):1323–1332.
- [19] Moran PAP. Random processes in genetics. *Mathematical Proceedings of the Cambridge Philosophical Society*. 1958;54(1):60–71.
- [20] Ewens WJ. *Mathematical Population Genetics*. Springer-Verlag; 1979.
- [21] Myers J, Clark LB. Culture conditions and the development of the photosynthetic mechanism: II. An apparatus for the continuous culture of *Chlorella*. *J Gen Physiol*. 1944 Nov;28(2):103–112.
- [22] Weissman DB, Desai MM, Fisher DS, Feldman MW. The rate at which asexual populations cross fitness valleys. *Theor Pop Biol*. 2009;75:286–300.
- [23] Traulsen A, Claussen JC, Hauert C. Coevolutionary dynamics: from finite to infinite populations. *Phys Rev Lett*. 2005 Dec;95(23):238701.
- [24] Traulsen A, Hauert C. Stochastic evolutionary game dynamics. In: Schuster HG, editor. *Reviews of Nonlinear Dynamics and Complexity*. vol. II. Wiley-VCH; 2009. .
- [25] Lipsitch M, Levin BR. The population dynamics of antimicrobial chemotherapy. *Antimicrob Agents Chemother*. 1997 Feb;41(2):363–373.
- [26] Wahl LM, Nowak MA. Adherence and drug resistance: predictions for therapy outcome. *Proc Biol Sci*. 2000 Apr;267(1445):835–843.
- [27] Wu Y, Saddler CA, Valckenborgh F, Tanaka MM. Dynamics of evolutionary rescue in changing environments and the emergence of antibiotic resistance. *J Theor Biol*. 2014 Jan;340:222–231.
- [28] Meredith HR, Lopatkin AJ, Anderson DJ, You L. Bacterial temporal dynamics enable optimal design of antibiotic treatment. *PLoS Comput Biol*. 2015 Apr;11(4):e1004201.
- [29] Abel Zur Wiesch P, Kouyos R, Abel S, Viechtbauer W, Bonhoeffer S. Cycling empirical antibiotic therapy in hospitals: meta-analysis and models. *PLoS Pathog*. 2014 Jun;10(6):e1004225.
- [30] Ke R, Loverdo C, Qi H, Sun R, Lloyd-Smith JO. Rational Design and Adaptive Management of Combination Therapies for Hepatitis C Virus Infection. *PLoS Comput Biol*. 2015 Jun;11(6):e1004040.
- [31] Schulz zur Wiesch P, Engelstadter J, Bonhoeffer S. Compensation of fitness costs and reversibility of antibiotic resistance mutations. *Antimicrob Agents Chemother*. 2010 May;54(5):2085–2095.
- [32] Bauer M, Graf IR, Ngampruetikorn V, Stephens GJ, Frey E. Exploiting ecology in drug pulse sequences in favour of population reduction. *PLoS Comput Biol*. 2017 Sep;13(9):e1005747.
- [33] Fisher DS. *Evolutionary Dynamics*. In: Bouchaud JP, Mézard M, Dalibard J, editors. *Les Houches, Session LXXXV, Complex Systems*. Elsevier; 2007. .
- [34] Rouzine IM, Rodrigo A, Coffin JM. Transition between stochastic evolution and deterministic evolution in the presence of selection: general theory and application to virology. *Microbiol Mol Biol Rev*. 2001 Mar;65(1):151–185.
- [35] Gutierrez S, Michalakis Y, Blanc S. Virus population bottlenecks during within-host progression and host-to-host transmission. *Curr Opin Virol*. 2012 Oct;2(5):546–555.

- [36] van Marle G, Gill MJ, Kolodka D, McManus L, Grant T, Church DL. Compartmentalization of the gut viral reservoir in HIV-1 infected patients. *Retrovirology*. 2007;4:87.
- [37] Nissen-Meyer S. Analysis of effects of antibiotics on bacteria by means of stochastic models. *Biometrics*. 1966;22(4):761–780.
- [38] Hansen E, Woods RJ, Read AF. How to Use a Chemotherapeutic Agent When Resistance to It Threatens the Patient. *PLoS Biol*. 2017 Feb;15(2):e2001110.
- [39] Melbinger A, Cremer J, Frey E. Evolutionary game theory in growing populations. *Phys Rev Lett*. 2010 Oct;105(17):178101.
- [40] Huang W, Hauert C, Traulsen A. Stochastic game dynamics under demographic fluctuations. *Proc Natl Acad Sci USA*. 2015 Jul;112(29):9064–9069.
- [41] Levin-Reisman I, Ronin I, Gefen O, Braniss I, Shoshani N, Balaban NQ. Antibiotic tolerance facilitates the evolution of resistance. *Science*. 2017 02;355(6327):826–830.
- [42] Bitbol AF, Schwab DJ. Quantifying the role of population subdivision in evolution on rugged fitness landscapes. *PLoS Comput Biol*. 2014 Aug;10(8):e1003778.
- [43] Nahum JR, Godfrey-Smith P, Harding BN, Marcus JH, Carlson-Stevermer J, Kerr B. A tortoise-hare pattern seen in adapting structured and unstructured populations suggests a rugged fitness landscape in bacteria. *Proc Natl Acad Sci USA*. 2015 Jun;112(24):7530–7535.
- [44] Cooper JD, Neuhauser C, Dean AM, Kerr B. Tipping the mutation-selection balance: Limited migration increases the frequency of deleterious mutants. *J Theor Biol*. 2015 Sep;380:123–133.
- [45] Zhang Q, Lambert G, Liao D, Kim H, Robin K, Tung C, et al. Acceleration of emergence of bacterial antibiotic resistance in connected microenvironments. *Science*. 2011;333(6050):1764–1767.
- [46] Greulich P, Waclaw B, Allen RJ. Mutational pathway determines whether drug gradients accelerate evolution of drug-resistant cells. *Phys Rev Lett*. 2012;109:088101.
- [47] Hermsen R, Deris JB, Hwa T. On the rapidity of antibiotic resistance evolution facilitated by a concentration gradient. *Proc Natl Acad Sci USA*. 2012;109:10775–10780.
- [48] Baym M, Lieberman TD, Kelsic ED, Chait R, Gross R, Yelin I, et al. Spatiotemporal microbial evolution on antibiotic landscapes. *Science*. 2016 09;353(6304):1147–1151.
- [49] Jacobs MR. Optimisation of antimicrobial therapy using pharmacokinetic and pharmacodynamic parameters. *Clin Microbiol Infect*. 2001 Nov;7(11):589–596.
- [50] Wielgoss S, Barrick JE, Tenaillon O, Cruveiller S, Chane-Woon-Ming B, Médigue C, et al. Mutation rate dynamics in a bacterial population reflect tension between adaptation and genetic load. *G3*. 2011;1:183–186.
- [51] Gao P, Nie X, Zou M, Shi Y, Cheng G. Recent advances in materials for extended-release antibiotic delivery system. *J Antibiot*. 2011 Sep;64(9):625–634.
- [52] Toprak E, Veres A, Michel JB, Chait R, Hartl DL, Kishony R. Evolutionary paths to antibiotic resistance under dynamically sustained drug selection. *Nat Genet*. 2011 Dec;44(1):101–105.
- [53] Taylor C, Iwasa Y, Nowak A. A symmetry of fixation times in evolutionary dynamics. *Journal of Theoretical Biology*. 2006;243:245–251.
- [54] Sekimoto K. *Stochastic Energetics*. Springer-Verlag; 2010.

- [55] Gardiner CW. Handbook of Stochastic Methods for Physics, Chemistry and the Natural Sciences. Springer; 1985.
- [56] Nowak MA, Komarova NL, Sengupta A, Jallepalli PV, Shih IM, Vogelstein B, et al. The role of chromosomal instability in tumor initiation. Proc Natl Acad Sci USA. 2002 Dec;99(25):16226–16231.
- [57] Weinreich DM, Chao L. Rapid evolutionary escape in large populations from local peaks on the Wrightian fitness landscape. Evolution. 2005;59:1175–1182.
- [58] Weissman DB, Feldman MW, Fisher DS. The rate of fitness-valley crossing in sexual populations. Genetics. 2010;186:1389–1410.

Supplementary Material

1 Table of notations

Notation	Definition
S	Sensitive microorganisms
R	Resistant microorganisms
C	Resistant-compensated microorganisms
T	Period of the alternations of absence and presence of antimicrobial
T_1	Duration of the phase without antimicrobial (for asymmetric alternations)
T_2	Duration of the phase with antimicrobial (for asymmetric alternations)
N	Population size
δ	Fitness cost of antimicrobial resistance
μ_1	Mutation rate from S to R
μ_2	Mutation rate from R to C
t_C^t	Total time of full resistance evolution (time until the C type fixes, starting from a population of S individuals)
t_R^a	Average time when R individuals first exist in the presence of antimicrobial, starting from a population of S individuals
t_C^a	Average time when the first C mutant whose lineage will fix appears, starting from a population of R individuals
τ_R^d	Average lifetime of the lineage of a single R mutant, until it disappears, in a population of S individuals, in the absence of antimicrobial
τ_R^f	Average fixation time of the lineage of a single R mutant in a population of S individuals, in the presence of antimicrobial
τ_C^f	Average fixation time of the lineage of a single C mutant in a population of R individuals
p_{SR}	Fixation probability of a single R mutant in a population of S individuals in the absence of antimicrobial
p_{RC}	Fixation probability of a single C mutant in a population of R individuals

Table S1: **Notations.** This table lists the different notations introduced in the main text and their meaning.

2 Fixation probabilities and fixation times in the Moran process

Here, we discuss in detail the fixation probabilities and mean fixation times in the Moran process, which are used throughout the main text. These quantities are already known [20, 24], but we present a derivation for the sake of pedagogy and completeness. Our derivation is based on the general formalism of first passage times, and gives the same results as those obtained in the literature, often using other methods [20, 24]. Next, we use the general expressions obtained to express the various fixation probabilities and fixation times used in the main text.

2.1 The Moran process

The Moran model [19, 20] is a simple stochastic process used to describe the evolution of the composition of asexual populations of finite and constant size. It allows one to incorporate variety-increasing processes such as mutation and variety-reducing processes such as natural selection.

In the Moran model, at each time step, an individual is chosen at random to reproduce and another one is chosen to die (see Figure S1). Hence, the total number of individuals in the population stays constant. Note that we will consider that the same individual can be selected to reproduce and die at the same step. Natural selection can be introduced by choosing the individual that reproduces with a probability proportional to its fitness. To implement mutations upon division, one can allow the offspring to switch type with a certain probability at each step. When a mutant arises within the Moran model at constant fitness, its lineage can either disappear or fix in the population, i.e. take over the whole population. The outcome is not fully determined by fitness differences as in a deterministic case, but also by stochastic fluctuations, also known as genetic drift. Here, we focus on the evolution of population composition under genetic drift and selection alone. In the rare mutation regime, these processes are much faster than the time between the occurrence of two mutations, so mutation can be neglected during the process of fixation of one type. The Moran model allows us to compute explicit expressions for quantities such as fixation probabilities and fixation times [20, 53] (see below).

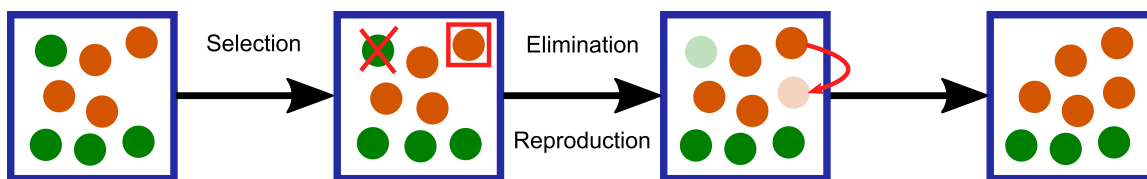


Figure S1: **Sketch of the Moran process.** One step of the Moran process is represented in a population with 8 individuals of 2 different types (different colors).

Let us consider a population of N individuals of two types A and B, which have fitnesses f_A and f_B , respectively. We denote the number of A individuals by j . Thus $N - j$ represents the number of B individuals. Let us study the evolution of j at one step of the Moran process (for an example, see Figure S1). The transition probabilities associated to the Moran process read [20]:

$$\begin{cases} \Pi_{j \rightarrow j+1} = \frac{N-j}{N} \frac{f_A j}{f_A j + f_B (N-j)} \\ \Pi_{j \rightarrow j-1} = \frac{j}{N} \frac{f_B (N-j)}{f_A j + f_B (N-j)} \\ \Pi_{j \rightarrow j} = 1 - \Pi_{j \rightarrow j+1} - \Pi_{j \rightarrow j-1} . \end{cases} \quad (\text{S1})$$

The Moran process is a discrete-time Markov process, since the probabilities of states j after one step only depend upon the present value of j . Let us take the limit of continuous time and write the master equation $\dot{\mathbf{P}} = \mathbf{R}_A \mathbf{P}$ giving the probability of being at state j at time t :

$$\frac{d}{dt} \begin{pmatrix} P_0 \\ P_1 \\ P_2 \\ \vdots \\ P_N \end{pmatrix} = \begin{pmatrix} -\Pi_{0 \rightarrow 1} & \Pi_{1 \rightarrow 0} & 0 & \cdots & 0 \\ \Pi_{0 \rightarrow 1} & -(\Pi_{1 \rightarrow 0} + \Pi_{1 \rightarrow 2}) & \Pi_{2 \rightarrow 1} & (0) & \vdots \\ 0 & \Pi_{1 \rightarrow 2} & -(\Pi_{2 \rightarrow 1} + \Pi_{2 \rightarrow 3}) & \ddots & 0 \\ \vdots & (0) & \ddots & \ddots & \Pi_{N \rightarrow N-1} \\ 0 & \cdots & 0 & \Pi_{N-1 \rightarrow N} & -\Pi_{N \rightarrow N-1} \end{pmatrix} \begin{pmatrix} P_0 \\ P_1 \\ P_2 \\ \vdots \\ P_N \end{pmatrix} . \quad (\text{S2})$$

This Markov chain has two absorbing states, namely $j = 0$ and $j = N$, which correspond to the fixation of B and A individuals, respectively. Once these states are reached, no more changes can occur, in the absence of mutation. It follows that all the components of the first and the last columns of \mathbf{R}_A equal to 0 (see Eq. S2), so \mathbf{R}_A is not invertible. In the following, we will denote by $\tilde{\mathbf{R}}_A$ the reduced transition rate matrix in which the rows and the columns corresponding to the absorbing states ($j = 0, j = N$) are removed, and by $\tilde{\mathbf{R}}_A^{-1}$ its inverse. Let us note that \mathbf{R}_A is a tridiagonal matrix, which allows for major simplifications of analytical calculations [20]. Note

that in order to obtain the transition rate matrix associated to B individuals, one just needs to apply the reversal $j \leftrightarrow N - j$. This corresponds to using the matrix $\mathbf{R}_B = \mathbf{J}\mathbf{R}_A\mathbf{J}$ where \mathbf{J} is the anti-identity matrix. For instance, in 2 dimensions, $\mathbf{J} = \begin{pmatrix} 0 & 1 \\ 1 & 0 \end{pmatrix}$.

2.2 General fixation probabilities and fixation times

Definitions. The fixation probability $\phi_{j_0}^A$ represents the probability that A individuals finally succeed and take over the population, starting from $j = j_0$ individuals of type A. In particular, $\phi_0^A = 0$ and $\phi_N^A = 1$. Similarly, $\phi_{j_0}^B$ is the fixation probability of the B individuals, still starting from $j = j_0$ individuals of type A.

Mean fixation times are the mean times to reach one of the absorbing states. The unconditional fixation time t_{j_0} is the average time until fixation in either $j = 0$ or $j = N$, when starting from a number $j = j_0$ of A individuals. The conditional fixation time $t_{j_0}^A$ corresponds to the average time until fixation in $j = N$, when starting from j_0 , provided that type A fixes. Note that in what follows, we will express the fixation times in numbers of steps of the Moran process. Conversion to generations can then be performed by dividing the number of Moran steps by N .

In the following, we present a derivation of the fixation probabilities and of the fixation times in the Moran process [20, 24] that uses the general formalism of mean first passage times [54].

Fixation probabilities. Assuming that at $t = 0$, the system is at state $j = j_0$, let us focus on the fixation probability $\phi_{j_0}^A$ of the A type in the population. The stochastic process stops at the time $\hat{\tau}_{FP}$ when j fixes, i.e. first reaches one of the absorbing states $\{j = 0, j = N\}$. Hence, integrating over all values of $\hat{\tau}_{FP}$, under the condition that fixation finally occurs in $j = N$, yields

$$\phi_{j_0}^A = \int_0^\infty p(\hat{\tau}_{FP} \in [t, t + dt] | j_0, j_\infty = N) = \Pi_{N-1 \rightarrow N} \int_0^\infty P_{N-1}(t) dt. \quad (\text{S3})$$

In the last expression, we have taken advantage of the fact that the only way to fix in $j = N$ between t and $t + dt$ is to be in state $j = N - 1$ at time t and then to transition from $N - 1$ to N (see Eq. S2). We have thus introduced the probability $P_{N-1}(t)$ of being in state $j = N - 1$ at time t , starting in state $j = j_0$ at time 0. More generally, the probability $P_i(t)$ can be considered.

Integrating the Master equation Eq. S2 to determine $P_i(t)$, with the initial condition $P_i(0) = \delta_{i j_0}$, where $\delta_{i j_0}$ denotes the Kronecker delta, which is equal to 1 if $i = j_0$ and 0 otherwise, yields

$$\phi_{j_0}^A = -\Pi_{N-1 \rightarrow N} (\tilde{\mathbf{R}}_A^{-1})_{N-1 j_0}. \quad (\text{S4})$$

A similar reasoning gives the fixation probability $\phi_{j_0}^B$ of the B type, still starting from j_0 individuals of type A and $N - j_0$ individuals of type B:

$$\phi_{j_0}^B = -\Pi_{1 \rightarrow 0} (\tilde{\mathbf{R}}_A^{-1})_{1 j_0}. \quad (\text{S5})$$

These two probabilities satisfy $\phi_{j_0}^A + \phi_{j_0}^B = 1$ since there are 2 absorbing states in the process.

Mean fixation times. Let us now focus on the mean fixation times, still assuming that at $t = 0$, the system is at state $j = j_0$. The probability that fixation in one of the absorbing states $\{j = 0, j = N\}$ occurs between t and $t + dt$ reads:

$$p(\hat{\tau}_{FP} \in [t, t + dt] | j_0) = \sum_{i=1}^{N-1} P_i(t) - \sum_{i=1}^{N-1} P_i(t + dt) = - \sum_{i=1}^{N-1} \frac{dP_i}{dt} dt, \quad (\text{S6})$$

where, as above, $P_i(t)$ represents the probability of being in state i at time t starting in j_0 at time 0 (note that the initial condition j_0 is omitted for brevity). Thus, the unconditional fixation

time can be expressed as:

$$t_{j_0} = \mathbb{E}[\widehat{\tau}_{FP} | j_0] = \int_0^\infty t p(\widehat{\tau}_{FP} \in [t, t + dt] | j_0) \quad (\text{S7})$$

$$= - \sum_{i=1}^{N-1} \int_0^\infty t \frac{dP_i}{dt} dt = \sum_{i=1}^{N-1} \int_0^\infty P_i(t) dt . \quad (\text{S8})$$

Here, we used Eq. S6, where the sums run over all the states that are not absorbing ($1 \leq i \leq N-1$). We also performed an integration by parts, and used $[t P_i(t)]_0^\infty = 0$ for $1 \leq i \leq N-1$, which holds because the probability of reaching an absorbing state of the Markov chain tends to 1 as $t \rightarrow \infty$. Integrating the Master equation Eq. S2 to determine $P_i(t)$, with the initial condition $P_i(0) = \delta_{i j_0}$, gives

$$t_{j_0} = - \sum_{i=1}^{N-1} (\widetilde{\mathbf{R}}_{\mathbf{A}}^{-1})_{i j_0} . \quad (\text{S9})$$

To express the conditional fixation time $t_{j_0}^A$ of type A, starting from j_0 A individuals, we need to take into account the condition that fixation finally occurs in state $j = N$:

$$p(\widehat{\tau}_{FP} \in [t, t + dt] | j_0, j_\infty = N) = \sum_{i=1}^{N-1} p(i | j_0, j_\infty = N)(t) - \sum_{i=1}^{N-1} p(i | j_0, j_\infty = N)(t + dt) . \quad (\text{S10})$$

The Bayes relation gives:

$$p(j | j_0, j_\infty = N) = \frac{\phi_j^A}{\phi_{j_0}^A} P_j . \quad (\text{S11})$$

By using the same method as for the unconditional fixation time, one obtains:

$$t_{j_0}^A = - \frac{1}{\phi_{j_0}^A} \sum_{i=1}^{N-1} \phi_i^A (\widetilde{\mathbf{R}}_{\mathbf{A}}^{-1})_{i j_0} . \quad (\text{S12})$$

Similarly, the conditional fixation time of the B type, starting from j_0 A individuals, reads:

$$t_{j_0}^B = - \frac{1}{\phi_{j_0}^B} \sum_{i=1}^{N-1} \phi_{N-i}^B (\widetilde{\mathbf{R}}_{\mathbf{B}}^{-1})_{i N-j_0} . \quad (\text{S13})$$

It is straightforward to verify that Eqs. S9, S12 and S13 are linked by the relation:

$$t_{j_0} = \phi_{j_0}^B t_{j_0}^B + \phi_{j_0}^A t_{j_0}^A . \quad (\text{S14})$$

Neutral drift. Let us first consider the case without selection $f_A = f_B$. In this case, the Moran process can be seen as a non-biased random walk, since individuals of both types are equally likely to be picked for reproduction and death. Fixation eventually happens due to fluctuations. This process, called neutral drift [20] corresponds to diffusion in physics. The transition rates of the system (S1) simplify as follows:

$$\begin{cases} \Pi_{j \rightarrow j+1} = \Pi_{j \rightarrow j-1} = \frac{j(N-j)}{N^2} \\ \Pi_{j \rightarrow j} = 1 - 2 \frac{j(N-j)}{N^2} . \end{cases} \quad (\text{S15})$$

Note that here, j can denote the number of A or B individuals indifferently. Indeed, the symmetry $j \leftrightarrow N-j$ entails $\mathbf{R}_{\mathbf{A}} = \mathbf{R}_{\mathbf{B}} = \mathbf{R}$, and the transition rate matrix is centrosymmetric, i.e. $\mathbf{R} = \mathbf{J} \mathbf{R} \mathbf{J}$. For consistency, we will continue to call j the number of A individuals.

The fixation probability $\phi_{j_0}^A$ can be obtained from Eq. S4. It involves elements of the inverse of the transition rate matrix. Solving $\widetilde{\mathbf{R}} \widetilde{\mathbf{R}}^{-1} = \mathbf{I}$, where \mathbf{I} is the identity matrix, gives

$$(\widetilde{\mathbf{R}}^{-1})_{N-1 i} = - \frac{i N}{N-1} \text{ for } 1 \leq i \leq N-1 . \quad (\text{S16})$$

Hence,

$$\phi_{j_0}^A = \frac{j_0}{N}. \quad (\text{S17})$$

Taking advantage of the centrosymmetry of \mathbf{R} (see above), a property which transfers to $\tilde{\mathbf{R}}$ and $\tilde{\mathbf{R}}^{-1}$, and entails $(\tilde{\mathbf{R}}^{-1})_{1j_0} = (\tilde{\mathbf{R}}^{-1})_{N-1N-j_0}$, we can apply Eq. S5, yielding

$$\phi_{j_0}^B = \frac{N-j_0}{N}. \quad (\text{S18})$$

Note that $\phi_{j_0}^A + \phi_{j_0}^B = 1$, as expected.

Let us now express the fixation times, focusing on the fate of a single mutant of type B, which corresponds to $j_0 = N - 1$. To compute the unconditional fixation time t_{N-1} , we again need elements of the inverse of the transition rate matrix (see Eq. S9), which are given by

$$(\tilde{\mathbf{R}}^{-1})_{iN-1} = -\frac{N}{N-i}. \quad (\text{S19})$$

Using Eqs. S9 and S19, we obtain:

$$t_{N-1} = N \sum_{i=1}^{N-1} \frac{1}{i}. \quad (\text{S20})$$

Similarly, using Eqs. S12, S17 and S19, we obtain the conditional fixation time of type A:

$$t_{N-1}^A = \frac{N^2}{N-1} \sum_{i=2}^N \frac{1}{i}. \quad (\text{S21})$$

Finally, using Eqs. S13, S17 and S19, and making use of the centrosymmetry of $\tilde{\mathbf{R}}^{-1}$ (see above), yields the conditional fixation time of type B:

$$t_{N-1}^B = N(N-1). \quad (\text{S22})$$

Selection. Let us now study the more general case involving selection. For this, let us consider two types A and B having different fitnesses f_A and f_B , and let us introduce $\gamma = f_A/f_B$. Note that with selection, the transition rate matrices \mathbf{R}_A and $\mathbf{R}_B = \mathbf{J}\mathbf{R}_A\mathbf{J}$ are different. In order to compute the fixation probability $\phi_{j_0}^A$, we need some elements of the inverse of the transition rate matrix $\tilde{\mathbf{R}}_A^{-1}$, which are given by:

$$(\tilde{\mathbf{R}}_A^{-1})_{N-1i} = -\frac{N}{N-1} \frac{1-\gamma^{-i}}{1-\gamma^{-N}} (N-1+\gamma^{-1}) \text{ for } 1 \leq i \leq N-1. \quad (\text{S23})$$

Then, using the previous result and Eq. S4, one obtains:

$$\phi_{j_0}^A = \frac{1-\gamma^{-j_0}}{1-\gamma^{-N}}, \quad (\text{S24})$$

and $\phi_{j_0}^A + \phi_{j_0}^B = 1$ yields:

$$\phi_{j_0}^B = \frac{1-\gamma^{N-j_0}}{1-\gamma^N}. \quad (\text{S25})$$

Let us now turn to the fixation times. According to Eq. S9, we need to compute other elements of the inverse of the transition rate matrix $\tilde{\mathbf{R}}_A^{-1}$. Those satisfy:

$$(\tilde{\mathbf{R}}_A^{-1})_{iN-1} = \frac{N}{i(N-i)} \frac{1-\gamma^i}{1-\gamma^N} (i-i\gamma-N) \text{ for } 1 \leq i \leq N-1. \quad (\text{S26})$$

Using Eqs. S9 and S26, the unconditional fixation time reads:

$$t_{N-1} = \frac{N}{1-\gamma^N} \sum_{i=1}^{N-1} \frac{(N+i\gamma-i)(1-\gamma^i)}{i(N-i)}. \quad (\text{S27})$$

To compute the conditional fixation time t_{N-1}^A , we substitute Eqs. S24 and S26 in Eq. S12, obtaining:

$$t_{N-1}^A = \frac{N}{(1-\gamma^N)(1-\gamma^{1-N})} \sum_{i=1}^{N-1} \frac{(N+i\gamma-i)(1-\gamma^i)(1-\gamma^{-i})}{i(N-i)}. \quad (\text{S28})$$

A similar reasoning can be used to obtain the conditional fixation time t_{N-1}^B starting from Eq. S13. In order to express the required $(\tilde{\mathbf{R}}_{\mathbf{B}}^{-1})_{j1}$, we combine the relation $\tilde{\mathbf{R}}_{\mathbf{B}} = \mathbf{J}\tilde{\mathbf{R}}_{\mathbf{A}}\mathbf{J}$, which implies $\tilde{\mathbf{R}}_{\mathbf{B}}^{-1} = \mathbf{J}\tilde{\mathbf{R}}_{\mathbf{A}}^{-1}\mathbf{J}$, together with Eq. S26, and obtain

$$(\tilde{\mathbf{R}}_{\mathbf{B}}^{-1})_{i1} = \frac{N}{i(N-i)} \frac{1-\gamma^{N-i}}{1-\gamma^N} (i\gamma-i-N\gamma) \text{ for } 1 \leq i \leq N-1. \quad (\text{S29})$$

This finally yields

$$t_{N-1}^B = \frac{N}{(1-\gamma^N)(1-\gamma)} \sum_{i=1}^{N-1} \frac{(N+i\gamma-i)(1-\gamma^i)(1-\gamma^{N-i})}{i(N-i)}. \quad (\text{S30})$$

2.3 Fixation probabilities and fixation times used in the main text

Let us now make an explicit link between the general expressions obtained above and the fixation probabilities and fixation times used in the main text.

Fixation probabilities. First, in the main text, p_{SR} represents the probability that a single resistant (R) mutant fixes without antimicrobial in a population of size N where all other individuals are of type S. Without antimicrobial, $f_{\text{S}} = 1$ and $f_{\text{R}} = 1 - \delta$. Considering S as type A and R as type B, we have $\gamma = f_{\text{S}}/f_{\text{R}} = 1/(1 - \delta)$, and our initial condition is $j_0 = N - 1$. Hence, Eq. S25 yields

$$p_{\text{SR}} = \phi_{N-1}^{\text{R}} = \frac{1 - (1 - \delta)^{-1}}{1 - (1 - \delta)^{-N}}. \quad (\text{S31})$$

In particular, in the effectively neutral case where $\delta \ll 1$ and $N\delta \ll 1$, it yields

$$p_{\text{SR}} \approx \frac{-\delta}{1 - e^{-N \log(1-\delta)}} \approx \frac{-\delta}{1 - e^{-N\delta}} \approx \frac{1}{N}, \quad (\text{S32})$$

i.e. we recover the result of the neutral case $\delta = 0$ (see Eq. S17). Conversely, in the regime where $\delta \ll 1$ and $N\delta \gg 1$, Eq. S31 yields

$$p_{\text{SR}} \approx \frac{-\delta}{1 - e^{-N\delta}} \approx \delta e^{-N\delta}. \quad (\text{S33})$$

Second, p_{RC} denotes the fixation probability of a single C individual in a population of size N where all other individuals are of type R. Independently of antimicrobial presence, $f_{\text{R}} = 1 - \delta$ and $f_{\text{C}} = 1$. Considering R as type A and C as type B, we have $\gamma = f_{\text{R}}/f_{\text{C}} = 1 - \delta$, and our initial condition is $j_0 = N - 1$. Hence, Eq. S25 yields

$$p_{\text{RC}} = \phi_{N-1}^{\text{C}} = \frac{\delta}{1 - (1 - \delta)^N}. \quad (\text{S34})$$

In particular, in the effectively neutral case where $\delta \ll 1$ and $N\delta \ll 1$, it yields

$$p_{\text{RC}} = \frac{\delta}{1 - e^{N \log(1-\delta)}} \approx \frac{\delta}{1 - e^{-N\delta}} \approx \frac{1}{N}, \quad (\text{S35})$$

i.e. we again recover the result of the neutral case $\delta = 0$ (see Eq. S17). Conversely, in the regime where $\delta \ll 1$ and $N\delta \gg 1$, Eq. S34 yields

$$p_{\text{RC}} \approx \frac{\delta}{1 - e^{-N\delta}} \approx \delta. \quad (\text{S36})$$

Finally, p_{SC} denotes the fixation probability of a single C mutant in a population of S individuals, without antimicrobial. In this case, $f_{\text{S}} = f_{\text{C}} = 1$, so we are in the neutral case, and Eq. S17 yields $p_{\text{SC}} = 1/N$.

Fixation times. First, $\tau_{\text{R}}^{\text{d}}$ denotes the average time it takes for the lineage of a single R mutant to disappear in the absence of antimicrobial. Hence, it is equal to the fixation time of the S type in a population that initially contains $N - 1$ individuals of type S and 1 individual of type R. Considering S as type A and R as type B, we have $\gamma = f_{\text{S}}/f_{\text{R}} = 1/(1 - \delta)$ without antimicrobial, and our initial condition is $j_0 = N - 1$, so $\tau_{\text{R}}^{\text{d}}$ is equal to t_{N-1}^{S}/N (see Eq. S28). Recall that t_{N-1}^{S} needs to be divided by the population size N because we expressed it in numbers of steps of the Moran process, while $\tau_{\text{R}}^{\text{d}}$ has to be expressed in numbers of generations. While the general formula Eq. S28 is rather complex, in the neutral case $\delta = 0$, it reduces to the much simpler expression in Eq. S21, which yields $\tau_{\text{R}}^{\text{d}} \approx \log N$ for $N \gg 1$. For $\delta > 0$, $\tau_{\text{R}}^{\text{d}}$ is shorter than in the neutral case, because the R mutants are out-competed by S individuals. Note that a good approximation to the exact formula in Eq. S28 can be obtained within the diffusion approach [20] (see the Fokker-Planck equation below).

Second, $\tau_{\text{R}}^{\text{f}}$ denotes the average time needed for the R mutants take over with antimicrobial, starting from one R mutant and $N - 1$ S individuals. Considering S as type A and R as type B, we have $\gamma = f_{\text{S}}/f_{\text{R}} = 0$ with antimicrobial, and our initial condition is $j_0 = N - 1$. Then $\tau_{\text{R}}^{\text{f}}$ is equal to t_{N-1}^{R}/N (see Eq. S30), with $\gamma = 0$. Using Eq. S30, we obtain

$$\tau_{\text{R}}^{\text{f}} = \sum_{i=1}^{N-1} \frac{1}{i}, \quad (\text{S37})$$

which entails $\tau_{\text{R}}^{\text{f}} \approx \log N$ for $N \gg 1$.

Finally, $\tau_{\text{C}}^{\text{f}}$ denotes the average time needed for the C mutants to take over, starting from one C mutant and $N - 1$ R individuals. Considering R as type A and C as type B, we have $\gamma = f_{\text{R}}/f_{\text{C}} = 1 - \delta$, independent whether antimicrobial is present or absent, and our initial condition is $j_0 = N - 1$. Hence, $\tau_{\text{C}}^{\text{f}}$ is given by t_{N-1}^{C}/N (see Eq. S30). In the neutral case $\delta = 0$, t_{N-1}^{C} reduces to Eq. S22, and thus $\tau_{\text{C}}^{\text{f}} \approx N$ for $N \gg 1$. For $\delta > 0$, it is shorter, as selection favors the fixation of C, and again a good approximation to the exact formula in Eq. S30 can be obtained within the diffusion approach [20] (see the Fokker-Planck equation below).

3 Large populations: deterministic limit

If stochastic effects are neglected, the dynamics of a microbial population can be described by coupled differential equations on the numbers of individuals of each genotype [20]. This deterministic approach is appropriate if the number N of competing microorganisms satisfies $N\mu_1 \gg 1$ [34]. Here, we derive and study the deterministic limit of the complete stochastic model studied in the main text.

3.1 From the stochastic model to the deterministic limit

Here, we present a full derivation of the deterministic limit of the stochastic model based on the Moran process (see above). This derivation closely follows those of Refs. [23, 24] and is presented here for the sake of pedagogy and completeness. Starting from the Master equation of our stochastic model, we obtain a Fokker-Planck equation, corresponding to the diffusion approximation [20], and then a deterministic differential equation, in the limits of increasingly large population sizes.

Let us first recall the Master equation corresponding to the Moran process, where j denotes the number of A individuals and $N - j$ the number of B individuals, as above:

$$\frac{dP_j(t)}{dt} = P_{j-1}(t) \Pi_{j-1 \rightarrow j} + P_{j+1}(t) \Pi_{j+1 \rightarrow j} - P_j(t) (\Pi_{j \rightarrow j-1} + \Pi_{j \rightarrow j+1}) . \quad (\text{S38})$$

The notations in Eq. S38 are the same as in the previous section, and time is expressed in number of steps of the Moran process. Let us now introduce the reduced variables $x = j/N$, $\tau = t/N$, as well as $\rho(x, \tau) = NP_j(t)$. Then, since one step of the Moran process occurs each time unit, Eq. S38 can be rewritten as:

$$\begin{aligned} \rho(x, \tau + 1/N) - \rho(x, \tau) &= \rho(x - 1/N, \tau) \Pi^+(x - 1/N) + \rho(x + 1/N, \tau) \Pi^-(x + 1/N) \\ &\quad - \rho(x, \tau) (\Pi^-(x) + \Pi^+(x)) , \end{aligned} \quad (\text{S39})$$

with

$$\Pi^-(x) = \Pi_{j \rightarrow j-1} = \frac{f_B x (1-x)}{f_A x + f_B (1-x)} \quad \text{and} \quad \Pi^+(x) = \Pi_{j \rightarrow j+1} = \frac{f_A x (1-x)}{f_A x + f_B (1-x)} . \quad (\text{S40})$$

Diffusion approximation. For $N \gg 1$, considering that jumps are small at each step of the Moran process, i.e. $1/N \ll x$ and $1/N \ll \tau$, the probability density $\rho(x, \tau)$ and the transition probabilities $\Pi^\pm(x)$ can be expanded in a Taylor series around x and τ . This expansion, known as a Kramers-Moyal expansion [55], yields, to first order in $1/N$:

$$\frac{\partial \rho(x, \tau)}{\partial \tau} = -\frac{\partial}{\partial x} [\rho(x, \tau) a(x)] + \frac{1}{2} \frac{\partial^2}{\partial x^2} [\rho(x, \tau) b^2(x)] \quad (\text{S41})$$

with

$$a(x) = \Pi^+(x) - \Pi^-(x) \quad \text{and} \quad b^2(x) = \frac{\Pi^+(x) + \Pi^-(x)}{N} . \quad (\text{S42})$$

Eq. S41 is known as a diffusion equation, or a Fokker-Planck equation, or a Kolmogorov forward equation [55], and $a(x)$ corresponds to the selection term (known as the drift term in physics), while $b^2(x)$ corresponds to the genetic drift term (known as the diffusion term in physics).

Deterministic limit. In the limit $N \rightarrow \infty$, retaining only the zeroth-order terms in $1/N$, Eq. S41 reduces to:

$$\frac{\partial \rho(x, \tau)}{\partial \tau} = -\frac{\partial}{\partial x} [\rho(x, \tau) a(x)] . \quad (\text{S43})$$

Let us focus on the average value of x , denoted by $\langle x \rangle$. Using Eq. S41 yields

$$\frac{d\langle x \rangle}{d\tau} = \int_0^1 \frac{\partial \rho(x, \tau)}{\partial \tau} x dx = - \int_0^1 \frac{\partial}{\partial x} [\rho(x, \tau) a(x)] dx \quad (\text{S44})$$

$$= - [x \rho(x, \tau) a(x)]_0^1 + \int_0^1 \rho(x, \tau) a(x) dx \quad (\text{S45})$$

$$= \langle a(x) \rangle \quad (\text{S46})$$

The first term of right hand side of Eq. S45 vanishes because $a(0) = a(1) = 0$. In the limit $N \rightarrow \infty$, the distribution of x is very peaked around its mean, so $\langle x \rangle \approx x$ and $\langle a(x) \rangle \approx a(x)$, yielding:

$$\frac{dx}{d\tau} = x(1-x) \frac{\Delta f}{\bar{f}} , \quad (\text{S47})$$

where $\Delta f = f_A - f_B$ denotes the difference of the fitnesses of the two types, while $\bar{f} = f_A x + f_B (1-x)$ is the average fitness in the population. Eq. S47 is an ordinary differential equation known as the adjusted replicator equation [23]. Recall that τ corresponds to the number t of steps of the Moran process divided by the total number N of individuals in the population.

Hence, τ is the time in numbers of generations used in the main text, and Eq. S47 is the proper deterministic limit for our stochastic process.

Note that in the framework of the Moran process, fitnesses are only relative. If one wanted to account for absolute fitness effects, so that a whole population reproduces faster if its average fitness is higher, one would need to include an additional rescaling of time $\tau' = \tau/\bar{f}$. Note that if \bar{f} is constant, this rescaling yields a standard replicator equation:

$$\frac{dx}{d\tau'} = x(1-x)\Delta f. \quad (\text{S48})$$

3.2 Deterministic description of the evolution of antimicrobial resistance

System of ordinary differential equations. Let us now come back to our model of the evolution of antimicrobial resistance, with three types of microorganisms (see Fig. 1A). In the limit of large populations, the complete stochastic model described in the main text will converge to a deterministic system of ordinary differential equations, as demonstrated above. Generalizing Eq. S48, by considering three types of individuals and taking into account mutations, yields a system of replicator-mutator equations [24]:

$$\begin{cases} \dot{s} = f_S(1-\mu_1)s - \bar{f}s \\ \dot{r} = f_R(1-\mu_2)r + f_S\mu_1s - \bar{f}r \\ s + r + c = 1, \end{cases} \quad (\text{S49})$$

where s , r and c are the population fractions of S (sensitive), R (resistant) and C (resistant-compensated) microorganisms, respectively, while f_S , f_R and f_C denote their fitnesses, $\bar{f} = f_Ss + f_Rr + f_Cc$ denotes the average fitness in the population, and dots denote time derivatives. To illustrate that Eq. S49 generalizes Eq. S48, consider the case where $c = 0$ and $\mu_1 = 0$: the first equation of Eq. S49 then yields $\dot{s} = f_Ss - [f_Ss + f_R(1-s)]s = s(1-s)(f_S - f_R)$. As demonstrated above, the deterministic limit of our stochastic model yields adjusted replicator equations (see Eq. S47). For the sake of simplicity, the present analytical discussion focuses on standard replicator equations (see Eq. S48).

The system of equations Eq. S49 only concerns population fractions, and constitutes the large-population limit $N \rightarrow \infty$ of our stochastic model at constant N . It is mathematically convenient to note that the same equations are obtained in the case of a population in which microorganisms have an exponential growth. This model, which enables us to recover the system S49, is governed by the following system of linear differential equations:

$$\begin{cases} \dot{N}_S = f_S(1-\mu_1)N_S \\ \dot{N}_R = f_R(1-\mu_2)N_R + f_S\mu_1N_S \\ \dot{N}_C = f_CN_C + f_R\mu_2N_R, \end{cases} \quad (\text{S50})$$

where N_S , N_R and N_C are the numbers of sensitive, resistant and resistant-compensated microorganisms, respectively. It is straightforward to show that the population fractions obtained from this exponential growth model satisfy Eq. S49: hence, this simple deterministic model allows one to understand the evolution of large microbial populations described by the Moran model (even though the total population is constant in the Moran model).

Analytical resolution. Being linear, the system in Eq. S50 is straightforward to solve analytically:

$$\begin{pmatrix} S \\ R \\ C \end{pmatrix} = \begin{pmatrix} 0 & 0 & 1 \\ 0 & 1 & \frac{f_S\mu_1}{f_S(1-\mu_1)-f_R(1-\mu_2)} \\ 1 & \frac{f_R\mu_2}{f_R(1-\mu_2)-f_C} & \frac{f_S\mu_1 f_R\mu_2}{(f_S(1-\mu_1)-f_R(1-\mu_2))(f_S(1-\mu_1)-f_C)} \end{pmatrix} \begin{pmatrix} \beta_1 e^{f_C t} \\ \beta_2 e^{f_R(1-\mu_2)t} \\ \beta_3 e^{f_S(1-\mu_1)t} \end{pmatrix} \quad (\text{S51})$$

where β_1 , β_2 and β_3 can be expressed from the initial conditions $S(0)$, $R(0)$ and $C(0)$. The fractions s , r and c can then be obtained from this solution, e.g. through $s = S/(S + R + C)$.

Limiting regimes and characteristic timescales. As in the main text, we are going to focus on the case where the population initially only comprises sensitive microorganisms, i.e. $s(0) = 1$. In the case of periodic alternations of absence and presence of antimicrobial, a small fraction of R microorganisms will appear within the first half-period without antimicrobial. The subsequent evolution of the population composition can be separated into three successive regimes. In the first one, it suffices to consider S and R microorganisms, as the fraction of C is negligible, because the appearance of C requires an additional mutation. The second regime is more complex, and involves all three types of microorganisms, as the growth of C microorganisms makes the fractions of S and R microorganisms decrease. Then, provided that antimicrobial has been present for a sufficient time, the fraction of S microorganisms becomes negligible, because they cannot divide with antimicrobial. Hence, the third regime only involves R and C microorganisms, and does not depend on the presence or absence of antimicrobial, because the fitnesses of R and C are unaffected. Here, we determine analytically the main timescales involved in these first and third regimes.

First regime: S vs. R. Let us consider the first regime where there are almost only S and R microorganisms. We are interested in the population fractions $s(t)$ and $r(t)$, with $s(t) + r(t) \approx 1$. Eq. S49 then gives:

$$\dot{s} = s(\Delta f_1 - s \Delta f_2), \quad (\text{S52})$$

where we have defined $\Delta f_1 = f_S(1 - \mu_1) - f_R$ and $\Delta f_2 = f_S - f_R$. Note that we expect $\Delta f_1 \approx \Delta f_2$, since biologically relevant values generally satisfy $\mu_1 \ll 1$ and $\mu_1 \ll \delta$. The solution of Eq. S52 reads

$$s(t) = \frac{s_0 e^{\Delta f_1 t}}{1 - s_0 \frac{\Delta f_2}{\Delta f_1} + s_0 \frac{\Delta f_2}{\Delta f_1} e^{\Delta f_1 t}}, \quad (\text{S53})$$

where s_0 is the fraction of S microorganisms at the beginning of the first regime (taken as $t = 0$ here). In the presence of antimicrobial ($f_S = 0$), the previous expression can be simplified, using $\Delta f_1 = \Delta f_2 = -(1 - \delta)$. This allows us to identify the characteristic time τ_1 of the decay of s , as R microorganisms take over:

$$\tau_1 = \frac{-1}{\Delta f_1} = \frac{1}{1 - \delta}. \quad (\text{S54})$$

The duration t_1 of the first regime in the presence of antimicrobial is governed by τ_1 . More precisely, Eq. S53 yields:

$$t_1 = \frac{1}{1 - \delta} \log \left(\frac{s_0(1 - s_1)}{s_1(1 - s_0)} \right), \quad (\text{S55})$$

where s_1 is the fraction of S microorganisms at the end of the first regime, at which point the fraction of C microorganisms is no longer negligible.

Third regime: R vs. C. Let us now turn to the third regime, assuming that antimicrobial has been present for a long enough time to allow S microorganisms to become a small minority. Eq. S49 then gives:

$$\dot{r} = r(\Delta f_3 - r \Delta f_4), \quad (\text{S56})$$

with $\Delta f_3 = f_R(1 - \mu_2) - f_C = -\delta(1 - \mu_2) - \mu_2$ and $\Delta f_4 = f_R - f_C = -\delta$, independently of whether antimicrobial is present or not. Again, we generally expect $\Delta f_3 \approx \Delta f_4$. The solution of Eq. S56 reads

$$r(t) = \frac{r_2(1 - \mu_2 + \mu_2/\delta) e^{-(\delta(1 - \mu_2) + \mu_2)t}}{1 - \mu_2 + \mu_2/\delta - r_2 + r_2 e^{-(\delta(1 - \mu_2) + \mu_2)t}} \underset{\substack{\mu_2 \ll 1 \\ \mu_2 \ll \delta}}{\approx} \frac{r_2 e^{-\delta t}}{1 - r_2 + r_2 e^{-\delta t}}, \quad (\text{S57})$$

where r_2 is the fraction of R microorganisms at the beginning of the third regime (taken as $t = 0$ here). Hence, the characteristic time τ_3 of the decay of r reads:

$$\tau_3 = \frac{1}{\mu_2 + \delta(1 - \mu_2)} \underset{\substack{\mu_2 \ll 1 \\ \mu_2 \ll \delta}}{\approx} \frac{1}{\delta}. \quad (\text{S58})$$

The duration t_3 of the third regime in the presence of antimicrobial is governed by τ_3 . More precisely, Eq. S57 yields:

$$t_3 \underset{\substack{\mu_2 \ll 1 \\ \mu_2 \ll \delta}}{\approx} \frac{1}{\delta} \log \left(\frac{r_2(1 - r_3)}{r_3(1 - r_2)} \right). \quad (\text{S59})$$

where r_3 is the fraction of R microorganisms at the end of this regime, when C has become dominant in the population.

Note that the timescales obtained here are governed by selection (through the relevant fitness differences δ and $1 - \delta$). This stands in contrast with the results from our stochastic model (see main text) where mutation rates are crucial, especially through the waiting time before resistant mutants appear. In the deterministic description considered here, small fractions of resistant mutants appear right away, so this consideration is irrelevant. However, mutation rates come into play in the durations of the different regimes within the deterministic model, through the fractions of each type of microorganisms at the beginning and at the end of each regime, but with a weak logarithmic dependence (see Eqs. S55-S59).

3.3 Comparison of stochastic and deterministic results

As in the main text, we now focus on the impact of a periodic presence of antimicrobial on the time it takes for a population to fully evolve resistance. For large microbial populations satisfying $N \gg 1/\mu_1$, we wish to check that the system of differential equations in Eq. S49 recovers the results obtained with our stochastic model. To this end, we solve the system in Eq. S49 numerically in the case of a periodic presence of antimicrobial. Note that complete fixation of a genotype does not happen in the deterministic model. Conversely, in the stochastic model, for a population of size N , the fixation of C corresponds to the discrete Moran step where the fraction c jumps from $1 - 1/N$ to 1. Hence, for our comparison between the deterministic results and the stochastic ones obtained for N microorganisms, we consider that C effectively fixes in the deterministic model when the fraction c reaches $1 - 1/N$. In addition, for exactness, we use a numerical resolution of the system in Eq. S49 where time is rescaled through $t \rightarrow t/\bar{f}$. Indeed, the proper deterministic limit of our stochastic model corresponds to modified replicator equations, such as Eq. S47 (see above).

Fig. S2 shows that the deterministic model yields results very close to those obtained through the stochastic model, in the case of large population sizes $N \geq 1/\mu_1$. We recover the regimes described in the main text, with a plateau for short periods, and a linear dependence on T for larger ones. Moreover, the relative error made by using the deterministic model instead of the stochastic one is less than $\sim 20\%$ (resp. $\sim 10\%$) for all data points with $N = 10^5$ (resp. $N = 10^6$) in Fig. S2.

Let us now present an analytical approximation for t_C^f , based on the different timescales computed previously. As the population is initially only composed of S microorganisms, they will remain dominant during the first half-period without antimicrobial, since they are fitter than R mutants (and we assume that $T/2$ is not large enough to extend to the point where C starts being important, which would then correspond to the valley crossing case). Afterwards, R microorganisms start growing fast during the second half-period. Note that in the deterministic case, there is always a nonzero fraction of resistant microorganisms at the end of the first half-period without antimicrobial, contrary to the stochastic case studied in the main text. Hence, we compute the fraction $s_0 = s(T/2)$ of S microorganisms at the end of the first half period, by using results for the above-described first regime without antimicrobials. This fraction $s_0 = s(T/2)$ is then taken as the initial condition of the first regime with antimicrobial. Then, for simplicity,

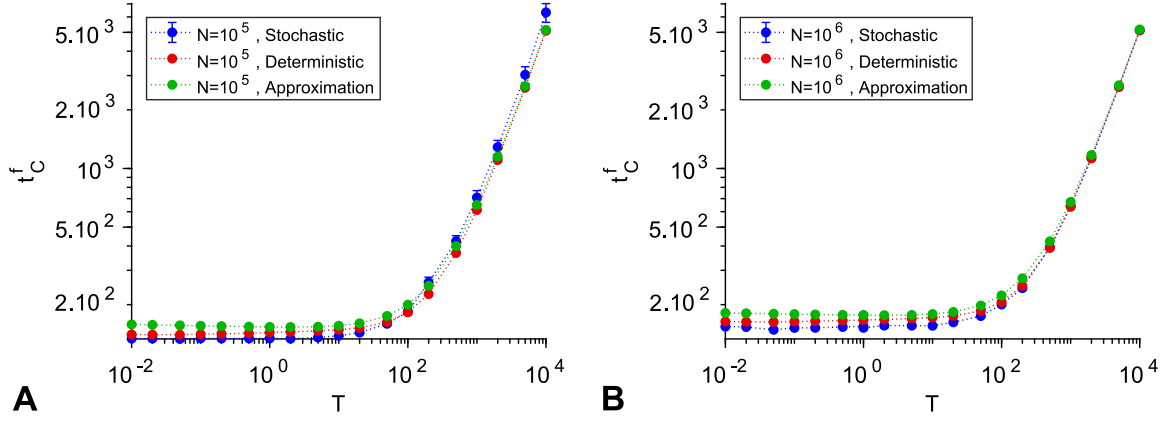


Figure S2: **Large populations: stochastic model vs. deterministic model.** The total time t_C^f of full resistance evolution is plotted versus the period T of alternations of absence and presence of antimicrobial, in the case of symmetric alternations. Results from simulations of the stochastic model (see Fig. 3A), numerical resolution of the deterministic model, and an analytical approximation of the deterministic solution (Eqs. S60-S61), are represented for $N = 10^5$ (A) and $N = 10^6$ (B). Parameter values: $\mu_1 = 10^{-5}$, $\mu_2 = 10^{-3}$, and $\delta = 0.1$.

we assume that s decays until it reaches $s_1 \approx 0.1$ (so $r_1 \approx 0.9$), while remaining in the first regime described above, in the presence of antimicrobial. We then assume the duration of the second regime is negligible, and consider that the third regime process starts right away, with a fraction $r_2 \approx 0.9$. As explained above, we consider that the third regime ends upon effective fixation of C, i.e. when c reaches $1 - 1/N$, which implies $r_3 = 1/N$. Using Eqs. S55 and S59, we obtain:

$$t_C^f \approx \frac{T}{2} + \frac{1}{1-\delta} \log \left(\frac{9s(T/2)}{1-s(T/2)} \right) + \frac{1}{\delta} \log(9(N-1)), \quad (\text{S60})$$

where $s(T/2)$ is obtained by using Eq. S53 in the absence of antimicrobial:

$$s(T/2) = \frac{e^{(\mu_2 + \delta(1-\mu_2) - \mu_1)T/2}}{1 - \frac{\mu_2 + \delta(1-\mu_2)}{\mu_2 + \delta(1-\mu_2) - \mu_1} (1 - e^{(\mu_2 + \delta(1-\mu_2) - \mu_1)T/2})}. \quad (\text{S61})$$

Eqs. S60-S61 yield good approximations of the analytical results obtained by numerical resolution of Eq. S49, as can be seen on Fig. S2. More precisely, the relative error made by using this approximation instead of the full numerical resolution is less than $\sim 13\%$ for all parameters in Fig. S2.

For $T \gg 2/\delta$, Eq. S61 reduces to $s(T/2) \approx 1 - \mu_1/[\mu_2 + \delta(1-\mu_2)] \approx 1 - \mu_1/\delta$, so only the first term in Eq. S60 then depends on T . Hence, this term becomes dominant for large T , yielding $t_C^f \approx T/2$ in this limit. This asymptotic behavior is again consistent with our predictions from the stochastic model (see main text). The horizontal purple solid line at large T in Fig. 3A, and the horizontal solid lines at large N in Fig. 3B, both correspond to $t_C^f \approx T/2$, showing excellent agreement with our stochastic simulations as well.

Conversely, for small periods, the first term of Eq. S60 can be neglected, so the dependence on T of t_C^f is weaker (Eq. S61 reduces to $s(T/2) \approx 1 - \mu_1 T/2$ for $T \ll 2/\delta$, so a weak logarithmic dependence on T remains, due to the second term of Eq. S60). It is interesting to note that the third term of t_C^f in Eq. S60 also increases logarithmically with N . This stands in contrast with the case of smaller populations, where our stochastic study showed that t_C^f essentially decreases linearly with N (see main text). This change of behavior as N increases can be seen on Fig. 3A in the regime of small T (in particular, for large N , the purple data points corresponding to $N = 10^6$ are then slightly higher than the blue ones corresponding to $N = 10^5$; see also Fig. S2, where the y-axis range and scale are the same on panels A and B).

4 Comparison to spontaneous fitness valley crossing

4.1 No antimicrobial: Crossing of a symmetric fitness valley

Let us compare the alternation-driven evolution of resistance to what would happen in the absence of alternations of phases of absence and presence of antimicrobial. If a population composed only of S (sensitive) microorganisms is subjected to a continuous presence of antimicrobial, it will not evolve resistance, because divisions are blocked (see Fig. 1A). Conversely, a population of S microorganisms that is never subjected to antimicrobial can spontaneously evolve resistance. In our model, this will eventually happen. This process is difficult and slow, because of the initial fitness cost of resistance: it requires crossing a fitness valley (see Fig. 1A). Fitness valley crossing has been studied in detail [22, 42, 56–58], but usually in the case where the final mutant has a higher fitness than the initial organism. In the evolution of antimicrobial resistance, compensatory mutations generally yield microorganisms with antimicrobial-free fitnesses that are similar to, but not higher than those of sensitive microorganisms [3, 4, 6]. Hence, we here extend the known results for fitness valley crossing by constant-size homogeneous asexual populations [22] to “symmetric” fitness valleys, where the final genotype has no selective advantage compared to the initial one. Briefly, the main difference with Ref. [22] is that the probability of establishment of the second mutant (C) in a population with a majority of non-mutants (S) is $1/N$ instead of being given by the selective advantage s of the second mutant. This probability plays an important role in the tunneling case.

There are two different ways of crossing a fitness valley. In *sequential fixation*, the first deleterious mutant fixes in the population, and then the second mutant fixes. In *tunneling* [56], the first mutant never fixes in the population, but a lineage of second mutants arises from a minority of first mutants, and fixes. For a given valley, characterized by δ (see Fig. 1A), population size N determines which mechanism dominates. Sequential fixation requires the fixation of a deleterious mutant through genetic drift, and dominates for small N , when stochasticity is important. Tunneling dominates above a certain N [22, 57]. Let us study these two mechanisms in the regime of rare mutations $N\mu_1 \ll 1$ where stochasticity is crucial.

In sequential fixation, the average time τ_{SF} to cross a valley is the sum of those of each step involved [22]. Hence $\tau_{\text{SF}} = 1/(N\mu_1 p_{\text{SR}}) + 1/(N\mu_2 p_{\text{RC}})$, where p_{SR} (resp. p_{RC}) is the fixation probability of a single R (resp. C) individual in a population of size N where all other individuals are of type S (resp. R). Fixation probabilities are known in the Moran process (see Supplementary Material, Section 2). In particular, if $N\delta \ll 1$ then $p_{\text{SR}} \approx p_{\text{RC}} \approx 1/N$ for our symmetric valley, so $\tau_{\text{SF}} \approx 1/\mu_1 + 1/\mu_2$ ($\approx 1/\mu_1$ if $\mu_1 \ll \mu_2$), while if $\delta \ll 1$ and $N\delta \gg 1$ then $p_{\text{SR}} \approx \delta e^{-N\delta}$ and $p_{\text{RC}} \approx \delta \gg p_{\text{SR}}$, so $\tau_{\text{SF}} \approx e^{N\delta}/(N\mu_1\delta)$.

In tunneling, the key timescale is that of the appearance of a successful first (R) mutant, i.e. a first mutant whose lineage will give rise to a second (C) mutant that will fix in the population [22]. Neglecting subsequent second mutation appearance and fixation times, the average tunneling time reads $\tau_{\text{T}} \approx 1/(N\mu_1 p_1)$, where p_1 is the probability that a first mutant is successful [22]. Upon each division of a first mutant, the probability of giving rise to a second mutant that will fix is $p = \mu_2 p_{\text{SC}}$, where p_{SC} is the fixation probability of a single C mutant in a population of S individuals. For our symmetric valley, $p_{\text{SC}} = 1/N$, so $p = \mu_2/N$. In the neutral case $\delta = 0$, Ref. [22] demonstrated that the first-mutant lineages that survive for at least $\sim 1/\sqrt{p}$ generations, and reach a size $\sim 1/\sqrt{p}$, are very likely to be successful, and fully determine the rate at which successful first mutants are produced. Since the lineage of each new first mutant has a probability $\sim \sqrt{p}$ of surviving for at least $\sim 1/\sqrt{p}$ generations [22], the probability that a first mutant is successful is $p_1 \sim \sqrt{p} \sim \sqrt{\mu_2/N}$. If $\delta > 0$, a first mutant remains effectively neutral if its lineage size is smaller than $1/\delta$ [22]. Hence, if $\delta < \sqrt{\mu_2/N}$, $p_1 \sim \sqrt{\mu_2/N}$ still holds. (This requires $N\mu_2 \gg 1$, otherwise the first mutant fixes before its lineage reaches a size $\sqrt{N/\mu_2}$.) Finally, if $\delta > \sqrt{\mu_2/N}$, the lineage of a first mutant will reach a size at most $\sim 1/\delta$, with a probability $\sim \delta$ and a lifetime $\sim 1/\delta$ [22], yielding $p_1 \sim \mu_2/(N\delta)$.

Given the substantial cost of resistance mutations ($\delta \sim 0.1$ [4, 6]) and the low compensatory mutation rates (in bacteria $\mu_2 \sim 10^{-8}$ [4]), let us henceforth focus on the case where $\delta > \sqrt{\mu_2/N}$

(which is appropriate for all $N \geq 1$ with the values mentioned). Then $\tau_T \approx 1/(N\mu_1 p_1) \approx \delta/(\mu_1 \mu_2)$, and two extreme cases can be distinguished:

(A) $N\delta \ll 1$ (effectively neutral regime): Then, $\tau_{SF} \approx 1/\mu_1$ (for $\mu_1 \ll \mu_2$) and $\tau_T \approx \delta/(\mu_1 \mu_2)$. Given the orders of magnitude above, generally $\delta > \mu_2$ in resistance evolution. Hence, sequential fixation is fastest, and the valley crossing time τ_V reads:

$$\tau_V = \tau_{SF} \approx \frac{1}{\mu_1}. \quad (\text{S62})$$

(B) $\delta \ll 1$ and $N\delta \gg 1$: Then,

$$\tau_V = \min(\tau_{SF}, \tau_T) \approx \min\left(\frac{e^{N\delta}}{N\mu_1\delta}, \frac{\delta}{\mu_1\mu_2}\right). \quad (\text{S63})$$

The transition from sequential fixation to tunneling [22] occurs when $N\delta e^{-N\delta} = \mu_2/\delta$.

We have focused on the rare mutation regime $N\mu_1 \ll 1$. If mutations are more frequent, the first successful lineage of R mutants that appears may not be the one that eventually fixes, so the valley-crossing time becomes shorter [22].

In Fig. 3B, the black simulation data points were obtained without any antimicrobial. The population then evolves resistance by valley crossing. The black curves correspond to our analytical predictions in Eq. S62 for $N \ll 1/\delta$ and in Eq. S63 for $N \gg 1/\delta$. In the latter regime, the transition from sequential fixation to tunneling occurs at $N \approx 65$ for the parameters of Fig. 3B. The agreement between simulation results and analytical predictions is excellent, with no adjustable parameter.

4.2 Alternation-driven process vs. valley-crossing process

Now that we have studied the spontaneous crossing of a symmetric fitness valley without any antimicrobial, let us come back to our periodic alternations of phases of absence and presence of antimicrobial. Resistance can then evolve by two distinct mechanisms, namely the alternation-driven process and the spontaneous valley-crossing process. It is important to compare the associated timescales, in order to assess which process will happen faster and dominate. This will shed light on the acceleration of resistance evolution by the alternations. For generality, we consider asymmetric alternations.

With alternations, spontaneous valley crossing can still happen, but new R lineages cannot appear with antimicrobial, because S individuals cannot divide (see Fig. 1A). Since the appearance of a successful R mutant is usually the longest step of valley crossing (see above), the average valley crossing time τ'_V with alternations will be longer by a factor T/T_1 than that without antimicrobial (τ_V), if more than one antimicrobial-free phase is needed to cross the valley, i.e. if $T_1 \ll \tau_V$. Eqs. S62 and S63 then yield

$$\tau'_V \approx \frac{T}{T_1\mu_1} \quad \text{for } N\delta \ll 1, \quad (\text{S64})$$

$$\tau'_V \approx \frac{T}{T_1} \min\left(\frac{e^{N\delta}}{N\mu_1\delta}, \frac{\delta}{\mu_1\mu_2}\right) \quad \text{for } \delta \ll 1 \text{ and } N\delta \gg 1. \quad (\text{S65})$$

Conversely, if $T_1 \gg \tau_V$, valley crossing generally happens within the first antimicrobial-free phase. Hence, the average valley crossing time τ_V is given by Eqs. S62 and S63. (Recall that the process is assumed to begin with an antimicrobial-free phase.)

We can now compare the timescales of the valley-crossing process to those of the alternation-driven process. For simplicity, let us assume that the dominant timescale in the latter process is the time t_R^a it takes to first observe an R organism in the presence of antimicrobial, i.e. $t_C^f \approx t_R^a$ (see Eq. 2). This is the case in a large and relevant range of parameters, especially if $\mu_1 \ll \mu_2$, as discussed above. Note also that the final step of fixation of the successful C lineage, which can become long in large populations (up to $\sim N$ in the neutral case, see Supplementary Material, Section 2), is the same in the alternation-driven process and in the valley-crossing process, so it

does not enter the comparison. The expression of t_R^a in Eq. 3 should thus be compared to the valley crossing time. If $T_1 \gg \tau_V$, valley crossing happens before any alternation, and is thus the relevant process, with time τ_V given by Eqs. S62 and S63. Let us now conduct our comparison of t_R^a and τ_V' for $T_1 \ll \tau_V$, where Eqs. S64 and S65 hold.

(A) If $T_1 \ll \tau_R^d$ (recall that τ_R^d is the average lifetime of an R lineage without antimicrobial, before it goes extinct): The alternation-driven process, with timescale $t_R^a = T/(N\mu_1 T_1)$ (see Eq. 3), dominates. Indeed, if $N\delta \ll 1$, τ_V' is given by Eq. S64, so for all $N > 1$, $t_R^a < \tau_V'$. And if $N\delta \gg 1$ and $\delta \ll 1$, Eq. S65 yields $t_R^a/\tau_V' \approx \delta e^{-N\delta} \ll 1$ in the sequential fixation regime, and $t_R^a/\tau_V' \approx \mu_2/(N\delta) \ll 1$ in the tunneling regime. Hence, if $T_1 \ll \tau_R^d$, the alternation-driven process dominates. Thus, alternations of absence and presence of antimicrobial strongly accelerate resistance evolution. For instance, in Fig. 3A, for $N = 100$ and $T/2 \ll \tau_R^d$, the alternation-driven process takes $t_R^a = 2/(N\mu_1) = 2 \times 10^3$ generations, while valley crossing takes $\tau_V = \delta/(\mu_1\mu_2) = 10^7$ generations without antimicrobial: alternations yield a speedup of 4 orders of magnitude. The speedup is even stronger for larger populations. Conversely, for $T_1 \ll T_2$, while the alternation-driven process is shorter than the valley-crossing process in the presence of alternations, it can nevertheless be longer than the valley-crossing process in the absence of antimicrobial. In this case, the drug actually slows down the evolution of resistance. When $T_1 \ll T_2$ and $T_1 \ll \tau_R^d$, in the tunneling regime, provided that $1/N \ll \delta \ll 2\sqrt{\mu_2/N}$, valley crossing takes $\delta/(\mu_1\mu_2)$ in the absence of antimicrobial (see Eq. S63), and $T_2\delta/(T_1\mu_1\mu_2)$ in the presence of alternations satisfying $T_1 \ll T_2$ (see Eq. S65). Meanwhile, the switch-driven process takes $T_2/(T_1N\mu_1)$ (see above). Hence, if $T_2 \gg T_1N\delta/\mu_2$, the alternation-driven process dominates, but it is slower than the valley-crossing process in the absence of antimicrobial: the drug then slows down resistance evolution. This effect can be seen on Fig. 4 for $T_1 \ll T_2$ and $T_1 \ll \tau_R^d$.

(B) If $T_1 \gg \tau_R^d$: Then $t_R^a = T/(N\mu_1\tau_R^d)$ (see Eq. 3). If $N\delta \ll 1$, valley crossing by sequential fixation is the dominant process. Indeed, Eq. S64 yields $t_R^a/\tau_V' \approx T_1/\tau_R^d \gg 1$. If $N\delta \gg 1$ and $\delta \ll 1$, Eq. S65 yields $t_R^a/\tau_V' \approx \delta e^{-N\delta} T_1/\tau_R^d$ in the sequential fixation regime, and $t_R^a/\tau_V' \approx \mu_2 T_1/(N\delta\tau_R^d)$ in the tunneling regime. A transition from the alternation-driven process to valley crossing occurs when these ratios reach 1. Qualitatively, if N is large enough and/or if T_1 is short enough, the alternation-driven process dominates.

For example, in Fig. 4A, parameters are such that the dominant mechanism of valley crossing is tunneling, so t_R^a/τ_V' reaches 1 for $T_1 = N\delta\tau_R^d/\mu_2 \approx 2.6 \times 10^5$ generations. This transition to the valley-crossing plateau is indeed observed for the curves with large enough T_2 . (Recall that if $T_2 \ll \tau_R^f$, extinction events occur when $T_1 \gg \tau_R^d$, see Fig. S3B.) The black horizontal lines in Figs. 4A and 4B correspond to our analytical prediction in Eq. S65, giving $\tau_V' \approx \delta/(\mu_1\mu_2)$ if $T_1 \gg \max(T_2, \tau_R^d)$. Similarly, in Fig. 3A, horizontal solid lines at large T correspond to the valley crossing times in Eqs. S64 or S65, depending on N . In Fig. 3B, in the regime of small N and large T , resistance evolution is achieved by tunneling-type valley crossing, yielding a plateau in the neutral regime $N \ll 1/\delta$ (see Eq. S64, plotted as a horizontal purple line) and an exponential increase for intermediate N (see Eq. S65). For larger N , we observe a T -dependent transition to the alternation-driven process, which can be fully understood using the ratio t_R^a/τ_V' (see above).

5 Detailed analysis of asymmetric alternations

5.1 Particular regimes

Here, we examine whether R mutants will fix during a single phase with antimicrobial, of duration T_2 . The fixation time of the lineage of an R mutant in the presence of antimicrobial is $\tau_R^f \approx \log N$ for $N \gg 1$ [20] (see above). If $T_2 \gg \tau_R^f$, fixation will happen within T_2 . In the opposite case, the fixation of R is not likely to occur within a single phase with antimicrobial. Two situations exist in this case (see Fig. S3).

(A) If $T_2 \ll \tau_R^f$ and $T_1 \ll \tau_R^d$ (Fig. S3A): The R lineage will drift for multiple periods, but its extinction is unlikely, as for symmetric alternations. This effect can induce a slight increase

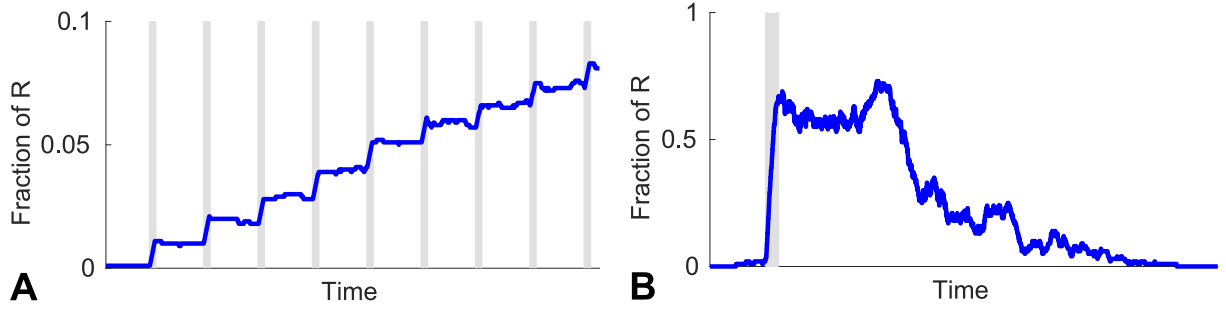


Figure S3: **Particular regimes.** The number of R individuals in the population is plotted versus time under alternations of phases without (white) and with antimicrobial (gray). Data extracted from simulation runs. (A) $T_2 \ll \tau_R^f$ and $T_1 \ll \tau_R^d$: the R lineage drifts for multiple periods. Parameters: $N = 10^3$, $T_1 = 10^{-1}$, $T_2 = 10^{-2}$. (B) $T_2 \ll \tau_R^f$ and $T_1 \gg \tau_R^d$: the R lineage goes extinct. Parameters: $N = 10^2$, $T_1 = 10^2$, $T_2 = 1$. In both (A) and (B), $\mu_1 = 10^{-5}$, $\mu_2 = 10^{-3}$ and $\delta = 0.1$.

of the total time of resistance evolution, which is usually negligible.

(B) If $T_2 \ll \tau_R^f$ and $T_1 \gg \tau_R^d$ (Fig. S3B): The R lineage is likely to go extinct even after it has started growing in the presence of antimicrobial. This typically implies $T_1 \gg T_2$, since $\tau_R^f \approx \log N$ and $\tau_R^d \lesssim \log N$ for $N \gg 1$ (see above). Hence, this case is specific to (very) asymmetric alternations. Spontaneous valley crossing then becomes the fastest process of resistance evolution (see Supplementary Material, Section 4).

5.2 Varying T_2 at fixed T_1

In the main text, we present a detailed analysis of what happens when T_1 is varied at fixed T_2 (see Fig. 4A). Here, we present a similar analysis if T_2 is varied at fixed T_1 . Fig. 4B shows the corresponding simulation results, together with our analytical predictions from Eqs. 2 and 3. In particular, a minimum is observed in Fig. 4B when varying T_2 for $T_1 \gg \tau_R^d$:

- When $T_2 \ll \tau_R^d \ll T_1$, valley crossing dominates.
- When $\tau_R^d \ll T_2 \ll T_1$, Eq. 3 gives $t_R^a = T/(N\mu_1\tau_R^d) \approx T_1/(N\mu_1\tau_R^d)$, which is independent from T_2 .
- As T_2 is further increased, $t_R^a = T/(N\mu_1\tau_R^d)$ increases, becoming proportional to T_2 when $T_2 \gg T_1$.

Hence, the minimum of t_R^a is $T_1/(N\mu_1\tau_R^d)$ and is attained for $\tau_R^d \ll T_2 \ll T_1$. In the opposite case where $T_1 \ll \tau_R^d$, Eq. 3 still gives $t_R^a = T/(N\mu_1T_1)$. Thus, t_R^a reaches a plateau $t_R^a = 1/(N\mu_1)$ for $T_2 \ll T_1 \ll \tau_R^d$, which means that the first R mutant yields the full evolution of resistance (as seen above). Then, t_R^a becomes proportional to T_2 for $T_2 \gg T_1$. Note that valley crossing is always slower than the alternation-driven process when $T_1 \ll \tau_R^d$ (see above), so no plateau is expected at large T_2 in this case.

6 Robustness of the binary antimicrobial action model

Throughout our study, we have modeled the action of the antimicrobial in a binary way: below the MIC (“absence of antimicrobial”), growth is not affected, while above it (“presence of antimicrobial”), sensitive microorganisms cannot grow at all (see Model section in the main text). The relationship between antimicrobial concentration and microorganism fitness is termed the pharmacodynamics of the antimicrobial [16, 49]. Our binary approximation is motivated by the usual steepness of pharmacodynamic curves around the MIC [16]. However, this steepness is

not infinite, and it is different for each antimicrobial. Here, we investigate the robustness of our binary model.

If one goes beyond the binary model and accounts for the smoothness of the pharmacodynamic curve, one additional factor enters the determination of the time dependence of fitness. It is the time dependence of the antimicrobial concentration, typically in a treated patient, which is known as pharmacokinetics [16, 49]. In fact, the time dependence of the fitness of sensitive microorganisms will be determined by a combination of pharmacodynamics and pharmacokinetics. Experimental pharmacodynamic curves are well-fitted by Hill functions, and pharmacokinetic curves are often modeled by exponential decays of drug concentration after intake [16]. The fitness versus time curve upon periodic antimicrobial intake will be a smooth periodic function resulting from the mathematical function composition of these two empirical relationships. The main feature of this curve will be how smooth or steep it is, which can be characterized by its rise time, i.e. the time it takes to rise from a value of f_S close to 0 to one close to 1. Recall that the fitness f_S of sensitive microorganisms ranges between 0 at very high antimicrobial concentrations and 1 without antimicrobial. In practice, we chose to define the rise time as the time taken to rise from $f_S = 0.1$ to $f_S = 0.9$.

Thus motivated, we consider a smooth and periodic fitness versus time relationship $f_S(t)$ (see Fig. S4A), and we study the impact of the rise time Θ on the evolution of antimicrobial resistance in a microbial population. In practice, our smooth function, shown in Fig. S4A, is built using the error function $\text{erf}(x) = (2/\sqrt{\pi}) \int_0^x e^{-u^2} du$, such that over each period of duration T :

$$f_S(t) = 1 - \frac{1}{2} \left[1 + \text{erf} \left(\frac{2}{\Theta} \left(t - nT - \frac{T}{2} \right) \right) \right] \quad \text{if } nT + \frac{T}{4} \leq t < nT + \frac{3T}{4}, \quad (\text{S66})$$

$$f_S(t) = \frac{1}{2} \left[1 + \text{erf} \left(\frac{2}{\Theta} (t - nT - T) \right) \right] \quad \text{if } nT + \frac{3T}{4} \leq t < (n+1)T + \frac{T}{4}, \quad (\text{S67})$$

where n is a non-negative integer. In addition, we take $f_S(t) = 1$ for $0 \leq t \leq T/4$, i.e. we start without antimicrobial at $t = 0$, and the first decrease of fitness occurs around $t = T/2$, in order to be as close as possible to our binary approximation (see Fig. 1B). Finally, as an extremely smooth case, we consider the case of a fitness f_S modeled by a sine function of period T , with the same initial condition and phase as our function with variable smoothness.

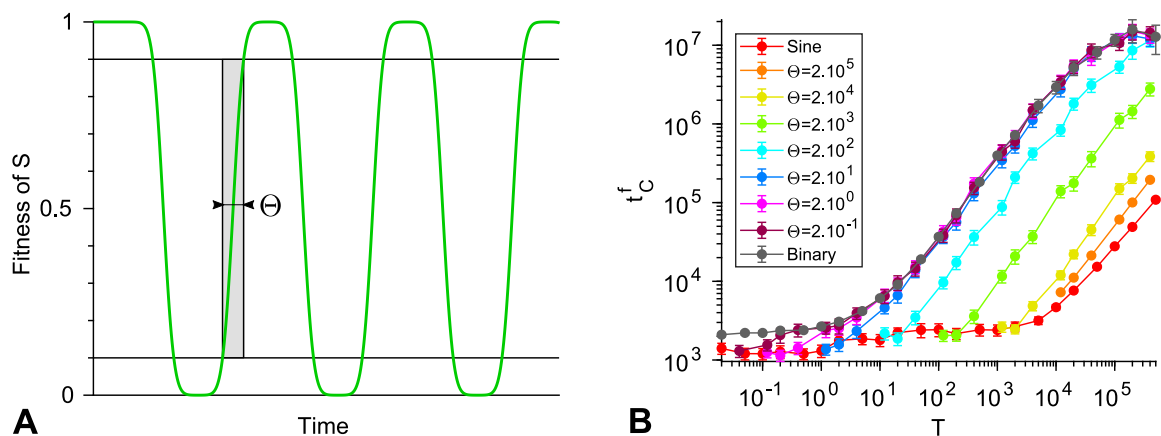


Figure S4: **Robustness of the binary antimicrobial action model.** (A) Smooth and periodic fitness versus time relationship considered: Θ denotes the rise time. (B) Total time t_C^f of full resistance evolution versus the period T for smooth alternations with different values of Θ , and for the binary model. Data points correspond to the average of simulation results (over 10 to 10^3 replicates), and error bars (often smaller than markers) represent 95% confidence intervals. Parameter values: $\mu_1 = 10^{-5}$, $\mu_2 = 10^{-3}$, $\delta = 0.1$, and $N = 100$.

We have performed stochastic simulations using the model described in the main text, but with the fitness versus time relationship given in Eqs. S66-S67. Fig. S4 shows that for small

rise times Θ , the dependence on the period T of the total time t_C^f of full resistance evolution is the same as with our binary approximation, provided that the rise time is much smaller than the period, $\Theta \ll T$. Conversely, for small Θ satisfying $\Theta \geq T$, in which case our function is very smooth even though the absolute rise time is short, the behavior of t_C^f is similar to that obtained for the sine function. For larger values of Θ , namely $\Theta \gg 10$, the binary case is no longer matched when $\Theta \ll T$, and instead, a behavior intermediate between the binary case and the sine case is observed. This intermediate behavior gets closer to that observed in the sine case as Θ is increased.

These results can be rationalized as follows. When Θ is smaller than the relevant evolutionary timescales identified in the main text (τ_R^d , τ_R^f and $1/(N\mu_1)$, the shortest ones being τ_R^d and τ_R^f for $N\mu_1 \ll 1$), no relevant evolutionary process can happen during a single smooth rise or decay of the fitness. If in addition Θ is much smaller than the environmental timescale T , then the fitness versus time function is steep and effectively binary. However, if Θ is not much smaller than T , then the function is smooth, and the binary approximation is inappropriate. Finally, if Θ is longer than the shortest relevant evolutionary timescales (τ_R^d , τ_R^f), then relevant evolutionary processes can happen within a single smooth rise or decay of the fitness, and the behavior is more complex. In a nutshell, our binary approximation is appropriate provided that the rise time satisfies $\Theta \ll \min(T, \tau_R^d, \tau_R^f)$.